



Oscillating retreat of the last British-Irish Ice Sheet on the continental shelf offshore Galway Bay, western Ireland

Callard, L., Ó Cofaigh, C., Benetti, S., Chiverrell, R., Van Landeghem, K. J. J., Saher, M., Livingstone, S. J., Clark, C. D., Small, D., Fabel, D., & Moreton, S. G. (2020). Oscillating retreat of the last British-Irish Ice Sheet on the continental shelf offshore Galway Bay, western Ireland. *Marine Geology*, 420, [106087].
<https://doi.org/10.1016/j.margeo.2019.106087>

[Link to publication record in Ulster University Research Portal](#)

Published in:
Marine Geology

Publication Status:
Published (in print/issue): 01/02/2020

DOI:
[10.1016/j.margeo.2019.106087](https://doi.org/10.1016/j.margeo.2019.106087)

Document Version
Author Accepted version

General rights
Copyright for the publications made accessible via Ulster University's Research Portal is retained by the author(s) and / or other copyright owners and it is a condition of accessing these publications that users recognise and abide by the legal requirements associated with these rights.

Take down policy
The Research Portal is Ulster University's institutional repository that provides access to Ulster's research outputs. Every effort has been made to ensure that content in the Research Portal does not infringe any person's rights, or applicable UK laws. If you discover content in the Research Portal that you believe breaches copyright or violates any law, please contact pure-support@ulster.ac.uk.

**Oscillating retreat of the last British-Irish Ice Sheet on the continental shelf offshore
Galway Bay, western Ireland**

S. Louise Callard^{1,*}, Colm Ó Cofaigh¹, Sara Benetti², Richard C. Chiverrell³, Katrien J.J. Van
Landeghem⁴, Margot H. Saher⁴, Stephen, J. Livingstone⁵, Chris D. Clark⁵, David Small¹, Derek
Fabel⁶, Steven G. Moreton⁷

¹ *Department of Geography, Durham University, Durham, DH1 3LE, UK*

² *School of Geography and Environmental Sciences, Ulster University, Coleraine, BT52 1SA,
Northern Ireland*

³ *School of Environmental Sciences, University of Liverpool, Liverpool, UK*

⁴ *School of Ocean Sciences, Bangor University, Menai Bridge, UK*

⁵ *Department of Geography, University of Sheffield, Sheffield, S10 2TN, UK*

⁶ *Scottish Universities Environmental Research Centre, University of Glasgow, East Kilbride,
G75 0QF*

⁷ *Natural Environment Research Council, Radiocarbon facility, East Kilbride, Scotland, G75
OQF, UK*

Abstract

During the Last Glacial Maximum, the British-Irish Ice Sheet extended across the continental
shelf offshore of Galway Bay, western Ireland, and reached a maximum westward extent on
the Porcupine Bank. New marine geophysical data, sediment cores and radiocarbon dates are
used to constrain the style and timing of ice-sheet retreat across the mid to inner-shelf.
Radiocarbon dated shell fragments in subglacial till on the mid-shelf constrains ice advance to
after 26.4 ka BP. Initial retreat was underway before 24.4 ka BP, significantly earlier than
previous reconstructions. Grounding-line retreat was accompanied by stillstands and/or

localised readvances of the grounding-line. A large composite Mid-Shelf Grounding Zone Complex marks a major grounding-line position, with the ice grounded and the margin oscillating at this position by, and probably after, 23 ka BP. The continental shelf was ice-free by 17.1 cal. ka BP, but the ice sheet may have retained a marine margin until c. 15.3 ka BP. Retreat occurred in a glacimarine setting and the ice sheet was fringed by a floating ice-shelf. Collectively, this evidence indicates a dynamic and oscillatory marine-terminating ice sheet offshore of western Ireland during the last deglaciation.

Key words: Grounding Zone Wedges; British-Irish Ice Sheet; Ice Shelf; Glacimarine; Last Glacial Maximum; Ice-Sheet Retreat; Continental Shelf

1. Introduction

Reconstructions of former ice sheets provides analogues that are useful for testing the performance of numerical ice-sheet models that seek to predict ice-sheet response(s) to climate warming. During the Last Glacial Maximum (LGM), at least 50% of the British-Irish Ice Sheet (BIIS) was marine-based (Sejrup et al., 2016). The ice sheet was drained by several large ice streams and had a marine margin extending from the west Shetland Shelf in the north (Bradwell et al., 2008; Bradwell et al 2019) to the shelf-edge of the Celtic Sea in the south (Praeg et al., 2015; Scourse et al., 2019). This broad marine margin, bordering the North Atlantic, was sensitive to both oceanographic and climatic drivers as well as sea-level change (Knutz et al., 2001, 2007; Peck et al., 2006; Scourse et al., 2009). Within the last decade, seafloor mapping of the continental shelf offshore of Ireland and Britain have provided new geomorphic evidence of the extent and style of BIIS advance and retreat (e.g., Sejrup et al., 2005, Van Landeghem et al., 2009; Benetti et al., 2010; Dunlop et al., 2011; Ó Cofaigh et al., 2012;). More recently, sedimentological and geochronological investigations have provided important constraints on

both the timing and style of BIIS retreat across the continental shelf during the last glacial cycle (e.g., Peters et al., 2015, 2016; Praeg et al., 2015; Callard et al., 2018, Ó Cofaigh et al., 2019, Roberts et al., 2018 Scourse et al., 2019).

On the Atlantic continental shelf bordering Ireland, several studies have argued that the western margin of the last BIIS terminated at the shelf edge during the LGM (e.g., Sejrup et al., 2005; Benetti et al., 2010; Dunlop et al., 2010; Ó Cofaigh et al., 2012, 2019; C. Clark et al., 2012; Peters et al., 2015, 2016; Praeg et al., 2015; Callard et al., 2018; Scourse et al., 2019). Ice rafted debris (IRD) records from deep sea cores collected along the western Atlantic margin of the BIIS imply that the ice sheet had attained a shelf-edge position by ~27 to 26.5 ka BP (Knutz et al. 2001; Peck et al. 2006; 2007; Scourse et al., 2009). Further to the north, in the Malin Sea and offshore Donegal Bay NW Ireland, this maximum position occurred after 26.8-26.3 ka, BP with onset of ice-sheet retreat between 26.7-24.8 ka BP and the majority of the shelf ice free by 23 ka BP (Callard et al., 2018; Ó Cofaigh et al., 2019). To the southwest, the Irish Sea Ice Stream reached the shelf edge between 27-24 ka BP (Praeg et al., 2015; Scourse et al., 2019) which is in line with recent dating of the maximum limit on the Isles of Scilly (Smedley et al., 2017). In the Irish Sea sector this was followed by rapid ice stream retreat by 25.1-24.2 ka (Small et al., 2018) with the ice stream margin in the northern Irish Sea Basin by 21.4 ± 1.0 ka BP (Chiverrell et al., 2013; 2018). Offshore of western Ireland, Peters et al. (2015, 2016) proposed an ice lobe that extended across Galway Bay and formed the western-most extent of the last BIIS, with geomorphic evidence of grounded ice out on the Porcupine Bank (Fig. 1), some 200 km from the Irish mainland. Peters et al. (2016) dated this advance to sometime after 24.1 ka BP and proposed late retreat of ice from the shelf with ice still grounded on the Porcupine Bank as late as 21.8 ka BP and only reaching the mid-shelf by 18.5 ka BP. This contrasts with results on the timing of ice sheet retreat from elsewhere along the western margin

(see above) and warrants further investigation to determine the relative importance of external vs. internal controls on the mechanisms behind the rapid retreat of marine-terminating ice sheets.

This paper presents new marine geophysical, sedimentological and geochronological data to reconstruct the pattern and timing of grounded ice on the mid-shelf between Galway Bay and the Porcupine Bank, offshore of western Ireland (Fig. 1). The objectives are to: 1) describe and characterise the glacial geomorphology on the mid and inner-shelf offshore Galway Bay, 2) to determine the nature of the depositional environments and style of ice sheet retreat, and 3) to provide a better-constrained retreat history for this sector of the British-Irish Ice Sheet across the mid to inner shelf.

2. Regional setting.

The study area lies offshore of counties Clare and Galway, central western Ireland and is confined to the shallow (<200m) mid to inner-shelf and the adjacent 0.5° slope of the Slyne Trough that forms a depression in the mid-shelf sea-floor (Fig. 1). This portion of the shelf extends and widens for up to 150 km westwards from the Irish coastline. Seismic reflection profiles show that the inner shelf is underlain by an offshore extension of the Precambrian metasedimentary rocks of Connemara and the Carboniferous limestone of the Clare Basin (Naylor et al., 1999) that lie close to, and crop out at, the seabed. Pliocene and Quaternary sediments overlie these basement bedrocks. The relatively flat sea-floor of the inner and mid-shelf is disrupted in the west by the Slyne Trough. This trough forms a gently sloping, 70 km wide depression in the mid-shelf. Seismic profiles of the eastern edge of the Slyne Trough, reveal a thick (160 m) sequence of Pliocene and Pleistocene sediments which are described as a proglacial fan by McCarron et al. (2018) (see below for more detail). The Slyne Trough

reaches depths of ~300 m bsl (below sea level) and links the mid-shelf to the Porcupine Bank on the outer-shelf. Porcupine Bank is a shallow, shelf-edge bank rising to a minimum of 145 m bsl, located 200 km due west of Ireland and is bounded to the north and west by the outer-shelf break at ~400 m bsl.

2.1. Glacial history

During the LGM the Irish Ice Sheet extended from the central Irish Midlands, Kerry-Cork Mountains and Connemara Mountains and converged in and across Galway Bay (Greenwood and Clark, 2009; Ballantyne and Ó Cofaigh., 2016). The offshore record of this sector of the BIIS has, until recently, been poorly constrained and our understanding has been reliant upon IRD records from deep sea cores collected south of the study site (core MD01-2461 Fig. 1; Peck et al 2006, 2007) and from the Donegal-Barra Fan to the north (e.g., Knutz et al 2001; Fig. 1). These IRD records imply that the BIIS had extended onto the continental shelf by 29 ka BP, and reached the shelf-edge by 27 to 26.5 ka BP. The IRD record from core MD01-2461 (Fig. 1) contains a constant, but variable, IRD flux between 26.5-17 ka BP, indicating both a persistent calving front but also evidence of destabilisation and readjustment of the marine margin throughout this period (Peck et al., 2006).

A number of recent marine geological and geophysical investigations on the continental shelf offshore western Ireland have extended our understanding of the glacial history of this region. On the Porcupine Bank (Fig. 1), Peters et al. (2015, 2016) mapped and dated a number of grounding-zone wedges (GZWs) on the basis of which they argued that grounded ice was positioned at the shelf edge as late as 25-24 ka BP with initial ice advance prior to this date. Inshore of the Porcupine Bank a large arcuate sediment ridge marks the mid-shelf grounding-line position (Fig. 1). This feature, termed the ‘Galway Lobe Grounding Zone Wedge’ by

Peters et al. (2015, 2016) (but referred to as the 'Mid-Shelf Grounding Zone Complex' in this study) was dated by Peters et al. (2015, 2016) who concluded that it marks a grounded ice margin dating to c. 21.2-18.5 ka BP. Further to the east, a second smaller sediment ridge marks a grounded ice margin on the mid-shelf at 18.5 ka BP with ice retreating inshore after this time (Fig 1). Based on these dates, Peters et al. (2016) concluded that retreat across the inner-mid shelf was rapid. In contrast, McCarron et al. (2018) argued that grounded ice did not extend onto the Porcupine Bank during the LGM, but rather was restricted to the 200 m isobath on the mid-shelf. The evidence for this is a thick sedimentary fan (termed the 'Connemara Fan' by McCarron et al., 2018) that lies seaward of this position and extends down into the Slyne Trough. Sub-bottom seismic data from the fan shows a series of stacked sediment layers that were likely deposited during multiple periods of ice occupancy of this grounding line position (see McCarron et al., 2018).

3. Methodology

Cruise JC106 of the *RRS James Cook* in August 2014 collected sub-bottom profiler (chirp) data and sediment cores (Fig. 1). The SBP120 chirp sub-bottom profiler is installed as an extension of the EM120 multibeam system, with frequency limits between 2.5 – 7 kHz and a maximum depth resolution of 0.3 ms. SBP profiles were visualised and interpreted using the IHS Kingdom™ software. To convert the two-way travel time to depth estimates in the sub-bottom profile data, we applied an average sound velocity of 1600 m s⁻¹ through marine sediments.

Eighteen vibrocores were retrieved (Table 1) using a British Geological Survey vibrocorer with a 6 m barrel and 8 cm core diameter. A further three piston cores up to 7.7 m long were taken from the inner shelf within 15 km of the Connemara coast using a UK National Oceanography Centre piston corer with a 12 cm diameter barrel. The underwater position of each core was

recorded using a Sonardyne Ranger USBL beacon attached to the corer. The on-board GEOTEK MSCL measured gamma density and magnetic susceptibility of each core at two centimetre resolution prior to splitting (results for each core are shown in Supplementary Information Figures 6 to 8). Shear vane measurements were made on the split core surface using a hand-held Torvane at 10 cm intervals. A GEOTEK XCT scanner provided X-radiographs on the split cores at a 92 μm resolution to further refine the core lithofacies. The X-radiographs, visual logs and physical properties were used to identify seven lithofacies (LF1-LF7).

From the cores a mixture of paired bivalves, mixed benthic foraminifera samples and shell fragments were collected and cleaned for radiocarbon dating. It is assumed that all dated material lived in a benthic and marine environment. Only whole, unabraded foraminifera specimens were picked from sieve (500, 180 and 63 μm) residues, with the assemblage dominated by the cold-water species *Elphidium clavatum*, *Cassidulina reniforme*, *Nonionella labradorica* and *Cibicides lobatulus*. Seventeen samples for radiocarbon dating (Table 2) were collected from cores on the shelf and mid-shelf slope of the Slyne Trough and submitted to the NERC Radiocarbon Facility for dating (SUERC publication codes) or the Keck C Cycle AMS laboratory, University of California, Irvine (UCIAMS publication codes) for ^{14}C dating. The primary aim of the dating was to constrain the timing of ice-sheet advance and retreat across the shelf. Our dating strategy was therefore threefold: (1) we dated reworked shell fragments in overconsolidated diamictos interpreted as subglacial tills to provide a maximum age on till formation and thus ice sheet advance; (2) we dated mixed benthic foraminifera samples and shell fragments from glaciectonised glaciarmine sediments. These dates constrain the timing of initial glaciarmine deposition and thus ice sheet retreat, but they also provide a maximum age for the subsequent glaciectonism and grounding-line oscillation/readvance; (3) we dated

shell and foraminiferal samples from deglacial glacimarine sediments to constrain the timing of ice sheet retreat. These samples were taken from as close to the transition with underlying subglacial sediments as possible or, where cores bottomed out in glacimarine sediments, we took the sample from as close as possible to the base of the core. The stratigraphic positions of the dates are shown and are discussed in context with the lithofacies interpretations (see Fig. 3, 6 and 8)

The conventional ^{14}C ages were calibrated using the Marine13 calibration curve with an inbuilt marine reservoir correction of 400 years and a ΔR of 0 years (Oxcal; Reimer et al., 2013). The ages are reported in the text as the calibrated 2σ median results (see Table 2). It is likely the samples would be subject to large and variable local ΔR during the LGM and late glacial period (e.g., Austin et al., 1995; Peck et al., 2006; Singarayer et al., 2008). We have applied two further age calibrations using the ΔR +300 and +700 yrs (c.f., Small et al., 2013; Table 2) as a sensitivity test. However, the different ΔR values has a modest impact and due to uncertainties in the correct reservoir age for this time period (Wanamaker et al., 2012) we have kept the ΔR of 0 in the text whilst acknowledging the caveat this could be significantly more.

4. Results and Interpretation

4.1. Acoustic Profiles

We present three acoustic profiles from the study area describing the major morphological features and acoustic signature of each. Where cores are available we also include brief reference to the associated sedimentary characteristics and we present full sedimentological descriptions in section 4.2.

4.1.1. Mid-inner shelf lines - description

Two acoustic profiles extend 150 km from the inner shelf westwards to water depths of 95-320 m. The northern profile from 0-39 km is characterised by a low gradient slope extending down into the Slyne Trough with a high amplitude seafloor reflector that is locally grooved (e.g., from 5-10 km and 16-22 km, Fig. 3a). The acoustic return beneath the seafloor appears to be relatively weak. Occasional point source reflectors are visible (e.g., at ~25 km). The sediments become more diffusely stratified with distance westwards and downslope (between 0-17 km). The slope is interrupted by a prominent topographic high between 18-22 km (Fig. 2a, 3a). Cores from this topographic high recovered predominantly massive pebbly mud (195VC and 196VC, Fig.3b), whereas a core from further upslope in 240 m water depth recovered clast-poor, laminated mud (194VC) (see section 4.2).

From 39 km westwards the seismic profile is characterised by a series of low relief and broad mounds (annotated as “M” in Figs. 2 and 4), at the seafloor. The eastern most mound (M1) at 39-72 km (Fig. 2a), is a multi-crested composite feature. Internally M1 is acoustically homogeneous. A core from this location recovered stiff, massive, matrix-supported diamicton overlain by bedded gravel and sand (193VC). To the east, these mounds transition into a series of 22 ridges that have a shorter wavelength (Fig. 4a) and are 5-9 m high and on average 720 m wide. These smaller ridges extend eastwards and beneath mound M2 (Fig. 2a, 4a). M2 (86.5-104 km; Fig. 2a, 4a) has a pronounced wedge-shaped geometry and is 23 m thick. M3 extends from 118-134 km (Fig. 2a) and shows some steeply dipping sub-seafloor reflectors. The final mound along the northern profile is M4 (Fig. 2a, 4c), which occurs from 132-136 km (Fig. 2a), is at least 19 m high and appears to be predominantly acoustically transparent.

Along the profile, acoustically stratified sediments infill small basins between the mounds described above (Fig. 2a, 4a). Stratification in these infills is variable, and up to 27 m thick.

225 The most prominent infill F1, occurs between mounds M1 and M2 from 73-90 km on the
226 profile, and onlaps both mounds (Fig. 2a, 4a). The lower half of the infill is acoustically
227 transparent and undulating, broadly conformable to the underlying smaller ridges (see above).
228 The infill becomes more stratified in the upper half. Stratification ranges from locally well-
229 developed but contorted in the deeper and central part of the basin fill, to more diffuse
230 elsewhere. At the eastern end of the F1 basin the acoustic stratification is interrupted by a lens
231 of predominantly transparent sediment. Faint internal reflectors are visible in places and the
232 lens is attenuated along profile to the west. Infill F2 occurs to the east of M2 and comprises 11
233 m of acoustically homogeneous sediment with, in places, faint internal reflectors. At the eastern
234 end of the profile (Fig. 2a, 4c) mound M4 is on-lapped to the west by hummocky-contorted
235 sediment (F3) which pinches out westwards. M4 is onlapped to the east by a basin fill of
236 acoustically stratified sediment 25 m thick with parallel internal reflectors (F4). Stratification
237 varies vertically from more continuous and well laminated to diffuse. A series of cores from
238 these basin fills recovered contorted, laminated silty muds (cores 191VC, 190VC, 189VC,
239 188VC and 186VC; Fig. 6) (see section 4.2).

240

241 The southern profile contains a series of mounds (M1 and M5-M7) extending west to east
242 across the shelf (Fig. 2b). The outermost mound M1 extends from 40-77 km, is multi-crested,
243 and 7-21 m high. This multicrested feature is a continuation of M1 identified in Figs. 2a and
244 4a and hence also named M1 in Figs. 2b and 5a. Cores from this mound comprised bedded
245 sand and gravel apart from 211VC, which recovered almost 2 m of massive diamicton (Fig. 6).
246 A series of buried, low amplitude ridges extend from 76-102 km and similar features are present
247 within M1 from 66-71 km (Fig. 2b, 5). At 102 km the reflector, which defines these buried
248 ridges, rises to the seabed. From 102-116 km eastwards there are a series of irregular,
249 undulating sub-bottom reflectors. These are overlain by mound M5. The eastern end of the

profile from 117-147 km is characterised by three well developed low amplitude mounds (M5-M7) which range from 10-19 m high and 5-13 km wide (Fig. 2b). M6 and M7 are internally homogeneous; M5 shows some faint, sub-horizontal internal reflections towards its western end.

As in the northern profile, acoustically stratified basin fills occur between several mounds (Fig. 2b). A basin fill occurs between 72 and 92 km, and it is ~7 m thick. Internally this is predominantly acoustically stratified, however, locally it contains discrete lenses of acoustically transparent sediment (Fig. 2b, 5). Towards the eastern end of the profile, a basin fill up to 5 m thick onlaps M6 and M7.

4.1.2. Mid-inner shelf lines – interpretation

Both mid-inner shelf acoustic profiles are characterised by a series of mounds separated by basin fills of variably stratified sediment. The mounds are low amplitude features but are typically wide (3 –15 km) and some have a distinct wedge-shaped geometry with their base defined by a sub-bottom reflector (e.g., M2 and M5). Internally they are predominantly acoustically homogeneous although in the case of M5 diffuse stratification is visible. These characteristics are consistent with an interpretation of the mounds as grounding-zone features formed during ice-sheet retreat. The distinct wedge-like geometry in some cases is consistent with grounding-zone wedges (GZWs) described from the literature (cf. Batchelor and Dowdeswell, 2015). The steeply dipping reflectors on M3 on the northern profile may record sediment progradation at the grounding-line or could alternatively reflect, at least in part, the presence of bedrock close to the seafloor. On both acoustic profiles, the outermost mound (M1) is multi-crested suggesting the grounding-line was oscillating on the outer shelf.

The low amplitude buried ridges on the outer shelf (see section 4.1 above) are present on both profiles and are an order of magnitude smaller than the bracketing larger GZWs (M1/M2 and M1/M5). Their dimensions are inconsistent with an origin as De Geer Moraines (cf. Todd et al., 2007). We interpret these ridges as recessional features formed by stillstands and/or minor oscillations of the grounding line during ice-sheet retreat (Shipp et al., 2002; Ó Cofaigh et al., 2012).

The acoustically stratified basin fills that occur between the mounds reflect sediment progradation beyond the grounding-line, most likely by a range of glacialmarine processes including sediment gravity flows, iceberg rafting and suspension settling from turbid meltwater plumes (Hogan et al., 2012, 2016). However, in some basins (F1 and F3) the sub-bottom reflectors are contorted and sediment cores from F1 recovered deformed, laminated muds. We suggest that this represents glacitectonism by grounded ice and provides further support for an oscillatory grounding line on the outer shelf. The transparent sediment lens at the eastern end of the F1 basin may be a debris flow sourced from the distal face of the GZW of M2 (c.f. Dowdeswell et al., 2010; Batchelor et al. 2011). However, it both rises and is attenuated westwards suggesting an alternative interpretation as a glacitectonic sediment raft (Evans, 2018). The distribution of mounds separated by stratified glacialmarine basin fills across the shelf indicates ice sheet retreat was episodic with occasional pauses and GZW/basin fill formation.

West of the outermost GZW (M1, Fig 1a and 3a) the slope extending down into the Slyne Trough exhibits diffuse acoustic stratification. This suggests sediment progradation into deeper water from a grounding line which delivered glacialgenic material downslope, most likely by sediment gravity flow processes (e.g. King et al., 1996; Stravers and Powell, 1997). However, the thick laminated mud sequences recovered in core 194VC implies deposition also involved

meltwater delivery. The seafloor incisions are consistent with iceberg scouring (Sacchetti et al., 2015; Thébaudeau et al., 2016).

4.1.3. Inner shelf offshore Connemara - description

A third sub-bottom profile, ~23.5 km in length and orientated SE-NW, was collected from 15 km offshore of the Connemara coast. The acoustic basement visible in the profile is regionally extensive and high amplitude (Fig. 7). It forms an irregular topography characterised by a series of highs, that crop out at the sea bed and intervening basins some of which contain sediment infills between 4-14 m thick (see below).

The basin infills are characterised by two distinct acoustic facies, which have a consistent vertical arrangement along the profile. The lower acoustic facies reaches up to 10 m thick and internally is variably acoustically stratified ranging from continuous horizontally layered sediments within the basins (e.g., location of core 184PC in Fig.7b), to contorted, disrupted and discontinuous internal reflectors (e.g., location of core 181VC in Fig. 7b). This unit was captured in four cores (180PC, 181VC, 183VC, 184PC) and comprises silty clay and clayey silt that is variably laminated-contorted (see section 4.2). The upper boundary of this acoustic facies is smooth to undulating and of medium to high strength. Where sampled this boundary comprises matrix-supported, poorly sorted, sandy gravel with abundant shell fragments.

The basin fills are capped by a well-developed, prominent acoustically transparent facies (Fig. 7). This reaches a maximum thickness of 11 m in the deepest basins. Cores from this facies recovered well sorted, saturated, silty sand that is massive and bioturbated. Its upper boundary is marked by a high amplitude, smooth reflector, which often forms the seafloor (Fig. 7).

4.1.4. Inner shelf offshore Connemara - interpretation

The acoustic basement visible in the profile is interpreted as bedrock on account of its high amplitude, distribution (both cropping out at seafloor and underlying stratified basin fills) and irregular form. The basin fills are consistent with formation in deglacial and postglacial environments. The lower acoustically stratified facies consist of laminated to contorted muds and is interpreted as a product of glacimarine sedimentation during ice sheet retreat (cf. Ó Cofaigh et al., 2016). These types of sediment are often produced by the rain-out of fine-grained sediment from suspension alternating with sediment gravity flow processes. Contorted bedding most likely reflects high sedimentation rates and the irregular topography that would have facilitated downslope resedimentation of fine-grained meltwater deposits (Hogan et al., 2012).

These glacimarine sediments are separated from the overlying acoustically transparent facies by poorly-sorted sandy gravel with abundant shells, which is interpreted as a lag deposit associated with bottom current reworking (Vianna et al., 1988). The overlying transparent facies comprises well sorted, saturated silty sands and are suggestive of a more quiescent depositional setting, most likely postglacial (Cooper et al., 2002).

4.2. Lithofacies descriptions

A total of twenty-one cores, three piston cores and eighteen vibrocores, were collected offshore of the Connemara coastline and across the slope and mid-shelf of Galway Bay. From these cores, we identify seven lithofacies (LF1-7) and describe these below.

4.2.1. LF1: Massive diamicton (Dmm) and minor stratified diamicton (minor Dms)

LF1 predominantly comprises massive, matrix-supported diamicton (Dmm). It is the basal lithofacies in six cores; two from the mid-shelf slope (195VC and 196VC, Fig. 3), three

(193VC, 187VC and 211VC Fig. 6) from the tops of the mid-shelf grounding-zone wedges (see section 4.1) and one from the inner shelf offshore of Connemara (181VC, Fig. 8). In core 191VC from a mid-shelf stratified basin fill, LF1 overlies laminated mud (LF2 and LF3).

In cores 195VC and 196VC from the mid-shelf slope LF1 is a dark grey (10YR 4/1), matrix-supported diamicton, with clay-silt matrix that contains abundant subrounded gravel to pebble-sized clasts. In 196VC LF1 is predominantly massive. Shear strengths in this core are 20-50 kPa increasing downcore (Fig. 3). In core 195VC, LF1 is also massive below 250 cm depth and shear strength values are generally greater than 60 kPa and reaching a maximum of 108 kPa at the base of the core. Above 250 cm depth in 195VC, however, LF1 ranges from massive to, locally, diffusely stratified. The diffuse stratification is localised, only visible in the x-radiographs and is imparted by sub-horizontal grain alignments and subtle textural variation (Fig. 9b, Supplementary Information Fig. 3). The shear strength of LF1 above 250 cm depth in this core is generally less than 30 kPa with a minimum of 10 kPa. Clast abundance of LF1 in cores 195VC and 196VC is variable. It is noticeably higher in 196VC (see x-ray Fig. 9a and Supplementary Information Fig. 3 and 4 for comparisons). The physical properties of Dmm in core 195VC and 196VC show a medium wet bulk density and magnetic susceptibility averaging 2.03 gr/mm and 104.3×10^{-5} SI respectively (see Supplementary Information for details).

Shell and coral fragments, and foraminifera are abundant throughout cores 195VC and 196VC. Radiocarbon dates on five shell fragments, four from 195VC and one from 196VC, constrain the age of LF1 (Table 2, Fig. 3). In core 195VC, three dates were obtained from the massive, stiff diamicton below 250 cm depth. A sample from 309-310 cm was beyond the range of radiocarbon dating but two further samples provided ages of 32994 ± 439 cal BP (SUERC-

60169) and 32407 ± 561 cal BP (SUERC-60168). A fourth sample at 219 cm depth from the softer massive to diffusely stratified diamicton dated 22849 ± 231 cal BP (SUERC-60165) (Table 2, Fig. 3). Finally, a shell fragment from 145-147 cm in core 196VC dated 15349 ± 204 cal BP (SUERC-60170).

In the mid-shelf cores and offshore Connemara, LF1 is a massive, matrix-supported diamicton with a clay-silt matrix. It is poorly sorted containing abundant gravel to granule-sized clasts including sub-rounded pebbles reaching up to 4 cm in diameter. The matrix is dark grey (5Y 4/1), predominantly massive, and contains occasional sandy pods and shell fragments. However, in core 211VC the matrix exhibits a gradational colour change downcore from dark grey (7.5 YR 4/2) to very dark grey (7.5 YR 4/1) and there is marked textural variation imparted by more clast-rich/gravelly zones. In core 191VC, LF1 is underlain by 27 cm of laminated mud (LF2) which becomes progressively more deformed (LF3) up-core forming a mixed or ‘amalgamation zone’ with LF1 (Fig. 9c, Supplementary Information Fig. 1). The upper boundary between LF1 and the overlying laminated mud of LF2 is sharp and the laminations are well preserved (Fig. 9d, Supplementary Information Fig. 1). In these mid-shelf cores, LF1 is very stiff with shear strength values ranging from 87 to 200 kPa. Overall, LF1 from the mid-outer shelf has a high wet bulk density and magnetic susceptibility averaging 2.15 gm/cc and 163.1×10^{-5} SI respectively (see Supplementary Information for details).

Four radiocarbon dates were obtained from LF1 on the mid-shelf. A shell fragment from 177 cm depth in core 191VC returned a non-finite age. The oldest age, from core 193VC is $26,446 \pm 284$ cal BP (SUERC-60164). A further two ages collected from core 211VC are $20,957 \pm 210$ cal BP (SUERC-60158) and $17,319 \pm 192$ cal BP (SUERC-60179) respectively.

4.2.2. LF2: Laminated mud (Fl)

LF2, laminated mud, occurs in six cores and consists of laminated clast-poor mud. In cores 180PC, 183VC and 184PC (Fig. 8) from offshore of Connemara on the inner shelf, LF2 forms the basal lithofacies; in core 181VC, LF2 overlies Dmm (LF1). It comprises the basal lithofacies in core 194VC (Fig. 3) from the mid-slope and also occurs in 191VC (Fig. 6) where it is interbedded with LF3 (Fl (def)) and LF1 (Dmm). LF2 comprises dark grey to very dark grey (5Y 3/1, 5Y 4/1) alternating horizontally laminated silts and clays. Individual laminae range from mm-cm thick. The upper and lower contacts vary from sharp, to diffuse and undulating. In some instances, the laminae have a wispy appearance (e.g., core 181VC, Fig. 9e). In core 184PC individual laminae become thicker and more diffuse up core. LF2 is predominantly clast free but locally may contain gravel- to granule-sized clasts that lie in discrete horizons (e.g., core 184PC Fig. 9h), or as occasional isolated pebbles (e.g., core 194VC Supplementary Information. Fig 2). Whole bivalves, abundant shell fragments and foraminifera are present throughout. Bioturbation is visible as burrows in the x-radiographs and as black mottles in core section but declines in frequency with depth downcore. Shear strengths in LF2 are variable. In core 194VC from the mid-slope LF2 is stiff, exhibiting shear strengths of 50-150 kPa. In core 191VC shear strengths of LF2 range from 60-90 kPa. This contrasts with cores from the inner shelf offshore Connemara where shear strengths measured in LF2 are much lower at 10-20 kPa. Wet bulk density is comparatively low, averaging 1.99 gm/cc whilst magnetic susceptibility is higher averaging 184.9×10^{-5} SI. However, when comparisons are made between areas, the average magnetic susceptibility is much higher from cores collected from offshore Connemara (180PC, 181VC, 183VC and 184VC) compared to the Fl captured on the mid-shelf (191VC and 194VC) with values averaging 260.6×10^{-5} SI and 75.9×10^{-5} SI respectively. This likely reflects a textural difference with the Connemara cores,

which lie close to the present-day shoreline, and have an increased sandy component compared to the mid-shelf cores (see Supplementary Information for details).

A sample of mixed benthic foraminifera from the base of 194VC dated 24361 ± 202 cal BP (SUERC-58323). A further three radiocarbon dates were obtained from samples from the bases of cores 180PC and 184PC. A sample of mixed benthic foraminifera from 180PC yielded a calibrated age of $16,962 \pm 214$ cal BP (SUERC-63562) while two articulated bivalves from the base of 184PC dated $17,101 \pm 270$ cal BP (UCAIMS-186921) and $17,101 \pm 247$ cal BP (UCAIMS-186924) respectively.

4.2.3. LF3: Deformed laminated mud (Fl (def))

LF3 comprises deformed laminated mud. It was recovered in seven cores from the slope (194VC, Fig. 3) and mid-shelf (186VC, 188VC, 189VC, 190VC, 191VC and 212VC, Fig. 6), and two cores from offshore Connemara (180PC and 184PC, Fig. 8). LF3 is a heavily deformed laminated mud (Fl (def)) that varies in nature spatially. In core 194VC Fl (def) is a stiff (24-56 kPa) colour mottled, silty clay and clayey silt containing water escape structures in the form of ball and pillow features that are visible in x-ray (Fig. 9g, Supplementary Information Fig. 2). Whole bivalves, shell fragments and foraminifera are present throughout as well as occasional small gravel-sized clasts. In core 194VC the deformed laminated mud of LF3 gradationally overlies the laminated mud of LF2.

Across the mid-shelf, Fl (def) is only recovered in cores from the basin infills and it forms the basal lithofacies of these cores. Here LF3 comprises a heavily deformed (e.g., 189VC, Fig. 9f), laminated fine sand and silty clay. Individual laminae/layers range from mm to 2 cm in thickness. The laminae have blurred upper and lower boundaries. The matrix varies in colour

with the fine sand units being black (5YR 2.5/2) and the silty clays being dark grey (10YR 4/1). In these mid-shelf cores, LF3 ranges from firm to stiff with shear strengths that range from a minimum of 17 kPa (core 190VC) to 88 kPa (Core 191VC). The wet bulk density for LF3 across the mid-shelf and Slyne Trough is high, averaging 2.11 gm/cc whilst magnetic susceptibility is medium averaging 131.8×10^{-5} SI (see Supplementary Information for details).

Three radiocarbon dates were obtained from LF3 in core 190VC. The dates are in reverse stratigraphic order (oldest at the top) and are $22,964 \pm 329$ cal BP (UCIAMS-164434) (192-194 cm), $25,414 \pm 241$ cal BP (UCIAMS-176384) (180-182 cm) and $27,267 \pm 202$ cal BP (SUERC-68873) (150-152 cm). A further date from LF3 in core 191VC returned an age beyond the range of radiocarbon dating.

In the two cores from the inner shelf offshore of Connemara LF2 consists of alternating beds of fine sand and clay-silt with abundant single and paired bivalves as well as shell fragments. These beds are contorted and show prominent development of sub-vertical to vertical wavy laminae consistent with water escape structures, as well as localised development of ball and pillow structures (Fig. 9). The boundaries of the individual laminae are often blurred and hard to discern. In both these cores LF3 exhibits localised zones of bioturbation in the form of Chondrites burrows. The matrix is soft to firm, with shear strength measurements not exceeding 20 kPa. The physical properties collected on these cores show a low average wet bulk density of 1.98 gr/mm but a very high magnetic susceptibility averaging 271×10^{-5} SI.

4.2.4. LF4: Massive mud (Fm)

LF4 is the basal lithofacies in core 186VC only (Fig. 6) and consists of a dark grey (2.5Y 4/1) clast-free, massive silty clay (Fm) that is very compact, increasing in shear strength from 70

kPa to 150 kPa. It contains occasional silt stringers and isolated zones of diffuse stratification towards the top of this bed that are only visible in the x-radiographs. LF4 was not dated. Both the wet bulk density and magnetic susceptibility are low, averaging only 1.98 gr/mm and 85.6×10^{-5} SI respectively, and contrast with the overlying Fl (def) (FF3) where these averages are considerable higher (see Supplementary Information for more detail). This is likely a result of the change in matrix with the overlying Fl (def) containing a large sand component.

4.2.5 LF5: Matrix-supported gravel (Gms)

LF5 is a matrix-supported gravel with a muddy-sandy matrix and abundant shell fragments (Gms). This lithofacies is poorly sorted with sub-rounded to sub-angular clasts that range in size from 0.5 to 3 cm in diameter. The upper and lower boundaries range from sharp to diffuse, and where overlain by LF7 (Sm) the boundary is often gradational. LF5 occurs in all the cores from the inner shelf offshore of Connemara forming a 10-70 cm thick unit that directly overlies LF3 or LF2 and is overlain in turn by LF7. LF5 was recovered in four cores on the inner- and mid-shelf (186VC, 192VC, 193VC and 208VC, Fig. 6). In these cores, individual beds of LF5 range in thickness from 10-44 cm and often have a sharp upper and lower boundary. The exception is core 193VC where the Gms of LF5 grades into the overlying LF7. The physical properties show high average values for both wet bulk density, 2.26 gr/mm, and magnetic susceptibility, 240.3×10^{-5} SI.

4.2.6. LF6: Clast supported gravel (Gm)

LF6 is identified in three cores from the outer mid-shelf (190VC 192VC and 193VC Fig. 6). LF6 comprises massive, clast-supported gravel (Gm) with clast size ranging from 0.5-4 cm in diameter. It forms the upper lithofacies in core 192VC. In core 193VC LF6 forms two beds; the lowermost is 20 cm thick and directly overlies LF1 whilst the second is interbedded with

the Gms of LF5 and is only 10 cm thick. Finally, a 12 cm thick bed directly overlying LF2 occurs in core 190VC. As expected with a large gravel component, both the wet bulk density and magnetic susceptibility are exceedingly high with average values of 2.45 gr/mm and 718.6×10^{-5} SI respectively.

4.2.7. LF7: Massive sand (Sm)

LF7 is the uppermost lithofacies in all cores collected in the study area, with the sole exception of 192VC. LF7 is a saturated, olive (5Y 4/3), massive, bioturbated fine to medium sand (Sm) containing abundant shell fragments and occasional gravel size clasts. The basal contact is sharp, convoluted and often truncates, mixes with or intrudes the underlying unit. LF7 is relatively thin in the slope and mid-shelf cores, ranging from 20 to 115 cm in thickness. In the cores from the inner shelf, offshore Connemara, LF7 ranges from 30 cm to a maximum of 480 cm in core 179PC. The wet bulk density is low, averaging 1.99 gr/mm whilst the magnetic susceptibility provides a medium average 124.45×10^{-5} SI. A basal radiocarbon age from a shell fragment in core 179PC provides a limiting age for this unit of $12,684 \pm 96$ cal BP (SUERC-63556).

4.3. Lithofacies Interpretations

4.3.1. LF1: Massive diamicton (Dmm) and minor stratified diamicton (minor Dms)

Massive, matrix-supported diamictons can be produced by several processes including debris flows (Eyles and Eyles 1989), iceberg rafting and scouring (Dowdeswell et al., 1994; Woodworth-Lynas and Dowdeswell, 1994), as well as subglacial deposition/deformation (Evans, 2018). The shear strengths of this lithofacies, however, are consistently high, in some cases reaching 210 kPa, implying they are overconsolidated. This is difficult to reconcile with an origin as a subaqueous debris flow or iceberg-rafted deposit produced by rain out through

the water column. Such processes would be much more likely to produce sediments with low shear strengths. Thus, the high shear strengths suggest that formation of LF1 involved sediment compaction. Massive diamictons with high shear strengths from glaciated continental shelves have often been interpreted as subglacial tills with the high shear strengths attributed to compaction by grounded ice (Wellner et al., 2001; Dowdeswell et al., 2004; Ó Cofaigh et al., 2005, 2013). This is our preferred interpretation for cores 193VC, 191VC, 187VC and the basal 160 cm of core 195VC. The deformed mud beneath LF1 in core 191VC also supports this interpretation. The presence of shell fragments in LF1 implies reworking of marine fauna. Dates on such reworked shells provide a maximum age for the enclosing till and thus for ice advance. Based on the date of 26.4 cal ka BP from the till in 193VC from the mid-shelf grounding-zone wedge (see section 4.2.1 above) this indicates that ice was grounded on the mid-shelf west of Ireland after 26.4 cal ka BP.

The massive diamictons in cores 211VC and 196VC are, however, more difficult to reconcile with an interpretation as subglacial till. In 211VC the youngest radiocarbon date from a reworked shell indicates diamicton formation after 17.3 cal ka BP. Similarly, a reworked shell in 196VC dated 15.3 cal ka BP. However, deglacial ages from the base of core 184PC from the inner shelf, 103 km further inshore of 211VC indicate that that site was ice free by at least 17.1 cal ka BP or even earlier (see section 4.3). It is therefore unlikely that the ice sheet was still grounded on the mid-shelf at this time. Taking into account both the high shear strengths of LF1 in 211VC and 196VC and the radiocarbon dates, we suggest that the massive diamicton in both these cores is most likely to be an iceberg turbate (cf. Woodworth-Lynas and Dowdeswell, 1994) with younger material being mixed into the underlying sediment, hence the young ages. Such scouring by the keels of grounded icebergs would be expected to deform and compact the surrounding sediment and offers a plausible explanation for the high shear

strengths in LF1. This interpretation is further supported by the seismic data that shows clear evidence of iceberg scouring on the bathymetric high, where core 196VC was located (Fig. 3).

In the upper 250 cm of core 195VC LF1 comprises matrix-supported diamicton that is predominantly massive but in places is diffusely stratified (minor Dms). The associated shear strengths are relatively low, particularly when compared to the subglacial tills described above. We interpret these characteristics as compatible with a subaqueous depositional environment at 22.8 cal ka BP in which sedimentation was by the rain-out of iceberg-rafted debris supplemented by suspension settling from turbid meltwater plumes (Dowdeswell et al., 1994, 2000; Cowan et al., 1997).

4.3.2. LF2: Laminated mud (Fl)

Laminated clast-poor muds with abundant marine fauna, including articulated bivalves and well preserved glacimarine foraminifera such as *E. clavatum* and *C. reniforme*, are indicative of meltwater-related sedimentation in a glacimarine environment (Lloyd et al., 2011; Jennings et al., 2017). They indicate that the core sites were free of grounded ice at the time of LF2 formation and thus that this lithofacies formed during ice-sheet retreat. Such laminated glacimarine muds can form by a range of processes including suspension settling from turbid overflow plumes (Cowan and Powell, 1990; Ó Cofaigh and Dowdeswell, 2001; Mugford and Dowdeswell, 2011) or deposition from fine-grained turbidity currents (Stow and Shanmugam., 1980). Laminae within 194VC are well preserved and in places have a wispy appearance with laminae boundaries sometimes blurred and hard to define. We suggest that these sediments are predominantly the result of suspension settling from turbid plumes (Hesse et al., 1997; Lucchi et al., 2013) with a minimal contribution from iceberg rafting. A basal date of 24.4 cal ka BP

from LF2 in the base of core 194VC shows that glacimarine conditions prevailed at this core site at that time and the site was free of grounded ice.

In contrast, the low shear strength laminated sequences from the cores on the inner shelf offshore Connemara show greater variability in terms of thickness, the occasional presence of load structures and clear normal grading as well as discrete granule horizons, characteristics which we suggest indicates that they formed, at least in part, from turbidity currents facilitated by the irregular topography of the inner shelf (Stow and Piper., 1984). The three dates from the bases of cores 180PC and 184PC indicate the inner shelf was free of grounded ice by at least 17.1 cal ka BP.

4.3.3. FL3: Deformed laminated mud (Fl (def))

Formation of the deformed laminated muds recovered from basin fills across the mid-shelf is inferred to have occurred in two-stages. The first stage involved deposition by a range of subaqueous processes similar to that producing the laminated muds of LF2 (see above). These muds were then deformed by an oscillating grounded ice margin. The evidence for this is fivefold: (i) the presence of contortion, load structures and water escape structures (e.g., 191VC, 190VC, 194VC); (ii) the facies relationship of LF2 and LF3 in which the deformed muds characteristically overlie undeformed laminated sequences. In core 191VC undeformed laminated muds are overlain by massive diamicton (LF1) and the transition between the two is marked by an amalgamation zone of deformed mixed sediment. This facies sequence is consistent with a glacitectorite-subglacial till origin in which laminated glacimarine sediments are overridden by grounded ice (cf. Ó Cofaigh et al., 2011; Evans 2018). Core 194VC shows a similar vertical transition from undeformed laminated mud (LF2) into heavily contorted muds; (iii) high shear strengths of up to 150 kPa of the deformed facies and, in some cases the

underlying laminated muds of LF2 (e.g., core 194VC), which is consistent with compaction by grounded ice; (iv) the sequence of three ages in the deformed facies of 190VC, which are in reverse stratigraphic order; and (v) interbedding of the deformed and undeformed laminated muds in several cores (191VC and 194VC). Collectively this indicates a dynamic, oscillating grounded ice sheet on the mid-shelf that deposited and then glacitected glacimarine sediments during episodic retreat across the shelf. This is consistent with the study of Peters et al. (2015, 2016) who interpreted the outermost and largest grounding-zone wedge on the mid-shelf as a composite feature produced during stillstand(s) and oscillations of grounded ice.

Chronological control on the age of LF3 and the oscillatory margin is provided by several dates from cores 190VC and 194VC on the mid-shelf and mid-shelf slope respectively. The date of 24.4 cal ka BP from the base of 194VC provides a maximum age on the overriding and deformation of the laminated glacimarine sediments in this core. Similarly, in core 190VC the youngest of the three dates (23 cal ka BP) from LF3 indicates that glacimarine sediments were overridden after this time.

Deformed laminated sediments of LF4 were also recovered from the inner-shelf offshore Connemara in cores 180PC and 184PC. These sediments are characterised by low shear strength not exceeding 20 kPa and contain frequent well preserved articulated bivalves (*Yoldiella* sp.) and bioturbation. We infer that these are glacimarine sediments that, in contrast to the mid-shelf, have not been overridden by grounded ice. Rather we attribute the deformation in these sediments to relate to mass movement in which glacimarine sediments deposited on an irregular inner shelf underwent downslope resedimentation.

4.3.4. LF4: Massive mud (Fm)

Lithofacies LF4 (massive mud) was only observed in a single core (186VC). The massive, fine-grained nature of LF4 is interpreted as indicative of a quiescent glacialmarine setting with sediment deposited by suspension-settling through the water column. The absence of clasts and bioturbation (burrows, mottling) suggests that iceberg delivery and/or IRD deposition and productivity were suppressed. This could be due to sedimentation in an ice-shelf cavity away from the grounding line (cf. Domack and Harris, 1988; Kilfeather et al., 2011) or the presence of sea ice fringing the ice-sheet margin (cf. Dowdeswell et al., 2000; Jennings et al., 2018). The high shear strengths that characterise this lithofacies (75-150 kPa) may reflect overriding by grounded ice similar to LF2 and LF3 above.

4.3.5. LF5, 6 and 7: Clast supported gravel (Gm), Matrix supported gravel (Gms) and Massive sand (Sm)

Massive gravel and sand units (LF5-7) form the upper lithofacies sequence in all cores collected from across the shelf. LF7 often overlies either a gravel lag or LF5 and/or LF6. This fining upward sequence of gravels (LF5), sandy gravels (LF6) to massive sands (LF7) that is seen in several cores (e.g., 193VC, 190VC, 186VC) is either evidence of a gradual weakening in bottom current activity, or alternatively represents a marine transgression and gradual increase in water depth (Vianna et al., 1998; Howe et al., 2001; Plets et al., 2015).

5. Discussion

5.1. Geomorphological and sedimentary signatures of the last British-Irish Ice Sheet on the Atlantic shelf west of Ireland

Over-consolidated subglacial tills in a series of cores (see section 4.3 above) indicate advance of the BIIS as a grounded ice mass across the continental shelf offshore of Galway Bay and western Ireland. A date on reworked shell from till in core 193VC provides a maximum age

for this advance and indicates that it occurred after 26.4 cal ka BP, and thus during the global LGM (gLGM) (26.5-19 cal ka BP; Clark et al., 2009). However, core 193VC only penetrated the upper few metres of the Mid-Shelf Grounding Zone Complex implying that much of this landform pre-dates the advance and was overridden by it. Hence, as McCarron et al. (2018) argue, the Mid-Shelf Grounding Zone Complex, may well be a product of more than one glacial cycle. The advance extended west of the Mid-Shelf Grounding Zone Complex, as indicated by the presence of subglacial till in core 195VC from the mid-shelf slope, and it grounded to at least 240 m water depth in the Slyne Trough. An extensive advance across the shelf is also supported by Peters et al. (2015, 2016) who document geomorphological and sedimentary evidence in the form of GZWs and subglacial till for grounded ice from the last glacial period further west on the Porcupine Bank. This contrasts with the interpretation of McCarron et al. (2018) who inferred the last ice sheet margin was restricted to the mid-shelf ('Irish Mainland Shelf').

Our seismic data indicate that retreat across the shelf was punctuated by stillstands and minor readvances of the grounding line. This is recorded by a series of large GZWs and intervening smaller moraines. The outermost GZW on the mid-shelf forms the large Mid-Shelf Grounding Zone Complex and is a composite, multi-crested feature, which contains overridden glacimarine muds on its eastern side implying an oscillatory grounding line. Basin fills between the GZWs across the shelf contain glacimarine sediments and are inferred to be a product of subaqueous sedimentation beyond the grounding-line when the ice sheet was positioned at a GZW. Hence, the basin fills are a product of time-transgressive deglacial glacimarine deposition. It is notable, however, that the basin fill sediments are often deformed and heavily consolidated indicating they have been overridden and glacitectonised, both on the mid-shelf and in the Slyne Trough (core site 194VC). Collectively this indicates that ice-sheet

retreat occurred in a glacimarine setting and was punctuated by readvances of the grounding line, which overrode and deformed these deglacial sediments (cf. Peters et al., 2016).

Although the GZWs and small moraines are both interpreted as deglacial landforms recording episodic, oscillatory, grounding-line retreat across the shelf, there is a marked contrast in size between them. The larger GZWs are several tens of kilometres wide and typically 10-20 m in amplitude. In contrast, the moraines are less than 1 km wide with amplitudes of 5-9 m, and in some cases are buried by the larger GZWs (Figs. 2, 4a, 4b, and see section 4.2 above). One interpretation for the contrast in size could be that the large GZWs are associated with deposition in a sub-ice shelf cavity, while the smaller ridges are a product of formation along a grounded tidewater ice front (Powell and Domack, 1995; Batchelor and Dowdeswell, 2015). We consider this unlikely, however, due to the intimate spatial relationship between these landforms on the mid-shelf whereby the smaller moraines occur between the larger GZWs and are in turn overprinted by them. A more likely explanation is that the stillstands which formed the smaller buried ridges were of shorter duration than those associated with the larger GZWs and/or were associated with lower sediment flux to the grounding-line.

5.2. Timing and dynamics of ice-sheet retreat

Radiocarbon dates from glacimarine sediments in our cores constrain the timing of ice sheet retreat across the shelf. The earliest date on retreat is from core 194VC from the Slyne Trough. Laminated glacimarine muds (LF2) from the base of the core dated 24.4 cal ka BP, showing that this site was ice-free by that time (Fig. 10). It also provides a maximum age on the subsequent readvance recorded in the upper part of 194VC (see section 4.3). This is significantly earlier than the date of ≤ 21.8 cal ka BP proposed for initial retreat from Porcupine Bank by Peters et al. (2016). Peck et al (2006) use peaks in BISS-sourced IRD as evidence for periods

of ice-marginal destabilisation. They show that the first increase in BIIS-IRD occurred from 26.2-25.8 ka BP, but that this was followed by a more prolonged interval of high BIIS-IRD flux between 25.5-23.4 which they relate to significant ice-marginal instability. This is broadly coincident with our interpretation of ice-sheet retreat and ice-free conditions occurring at core site 194VC by 24.4 ka BP.

The Mid-Shelf Grounding Zone Complex marks a major grounding-line position on the mid-shelf. A date of 23 cal ka BP from glacitected sediments in core 190VC from the east side of the moraine provides a maximum age for the most recent period of ice occupancy at the moraine. The geomorphology and glacitected sediments reflect the oscillatory grounding-line that advanced over and deformed these deglacial sediments. This is broadly consistent with ice-free conditions and glacial sedimentation dated to 22.8 cal ka BP on the slope of the Slynne Trough (core site 195VC). Additional constraint on the age of the Mid-Shelf Grounding Zone Complex is provided by two dates of 21.1 cal ka BP and 18.5 cal ka BP from benthic foraminifera in glacitected sediments from the flank of the moraine (Peters et al., 2016). This indicates the grounding-line was still occupying the Mid-Shelf Grounding Zone Complex at this time (Fig. 10) and deforming glacial sediments. Hence, the Mid-Shelf Grounding Zone Complex marks a prolonged stillstand of an oscillatory grounding-line on the mid-shelf. The flux of BIIS-derived IRD is variable throughout this period, possibly reflecting the oscillatory pattern of ice-marginal dynamics that we record on the shelf (c.f. Peck et al 2006, 2007).

The timing of ice sheet retreat and the subsequent grounding-line stabilisation at the Mid-Shelf Grounding Zone Complex coincides with both Greenland Interstadial 2 (GI2; ~22-24 ka BP) (Andersen et al., 2006), and the Heinrich 2 (H2) event that led to an abrupt rise in sea level at c. 24 ka BP (Siddall et al., 2003; Scourse et al., 2009). The climatic and oceanographic changes associated with GI2 and H2 are therefore potential external forcing mechanisms on ice sheet

dynamics on the Atlantic shelf offshore Galway Bay. However, the GZWs and smaller moraine ridges that we document across the mid-shelf point to numerous stillstands and readvances interrupting overall ice-sheet retreat. Hence, it is likely that internal mechanisms were also important controls on ice-sheet retreat dynamics. A well-known internal control on ice shelf and tidewater glacier dynamics that can act independently of climatic or oceanographic controls is sedimentation at the grounding line (Powell., 1991, Alley et al., 2007; Brinkerhoff et al., 2017). Where rates of sediment delivery to the grounding line are high, a positive feedback is introduced such that sediment deposition builds moraines or GZWs which in turn act to reduce water depth and thereby facilitate further grounding-line stabilisation and, in some cases, a short-lived readvance. Hence, while climate forcing is a plausible control on retreat dynamics across the mid-shelf given the available radiocarbon chronology, we suggest that localised internal glaciodynamic mechanisms related to sediment delivery at the grounding-line may also help to explain the numerous stillstands and the oscillatory behaviour at the Mid-Shelf Grounding-Zone Complex.

A date of 21 cal ka BP (core 211VC) from an iceberg turbate from west of the Mid-Shelf Grounding Zone Complex provides further constraint on ice-sheet retreat. It is possible that the ice sheet was still grounded at the Mid-Shelf Grounding Zone Complex at this time (Fig 10). Radiocarbon dates on deglacial sediments from offshore Connemara indicate that much of the shelf was ice-free by or before 17.1 cal ka BP (Fig. 10). There is no evidence of a significant readvance of the ice sheet onto the continental shelf after this time. Nevertheless, a date of 15.3 cal ka BP from iceberg turbate in core 196VC from west of the Mid-Shelf Grounding Zone Complex implies that icebergs were still transiting the shelf at this time, although the source of these bergs cannot be determined from the available data.

6. Conclusions

New acoustic stratigraphic, sedimentological and geochronological data from the continental shelf offshore central western Ireland provides new insights on the timing and style of ice sheet advance and retreat during the last glacial cycle. From the integrated analysis, a five-fold sequence of events is proposed below (see Fig. 10).

1. Ice sheet advance to a Mid-Shelf Grounding Zone Complex sometime after 26.4 cal ka BP. Subglacial till cored from within the Slyne Trough, at 240 m below sea-level, confirms that grounded ice extended beyond this mid-shelf position and likely grounded on the Porcupine Bank (cf. Peters et al., 2015).
2. Ice sheet retreat was underway before 24.4 cal ka BP as indicated by radiocarbon dated glacimarine sediments in the Slyne Trough. The timing of initial retreat is earlier than previously proposed for this region (Peters et al., 2015, 2016) but is consistent with dates on retreat from the Atlantic shelf further to the north and south (Callard et al., 2018; Ó Cofaigh et al., 2019; Scourse et al., 2019). It is also consistent with evidence of destabilisation of the BIIS from 25.5 to 24.1 ka BP based on the peak IRD flux in deep-sea core MD01-2461 (Peck et al., 2006, 2007).
3. Overconsolidated glacimarine sediments and subglacial tills in cores from the Slyne Trough record grounding-line readvance sometime after 24.4 cal ka BP.
4. Ice sheet retreat across the shelf was characterised by a dynamic and oscillating grounding-line as recorded by GZWs, moraines and deformed glacimarine sediments. Dating of over-consolidated glacimarine muds collected in this study combined with the chronology from Peters et al. (2016) indicate that grounded ice was still oscillating at the Mid-Shelf Grounding Zone Complex between 23-18.5 cal ka BP.

5. Most of the continental shelf was ice free by 17.1 cal ka BP. Evidence of iceberg
turbation at 15.3 ka BP implies a marine terminating margin at this time although we
found no evidence on the shelf for a re-advance of ice after 17.1 ka BP.

Acknowledgements

This research was funded by the UK Natural Environment Research Council grant; BRITICE-
CHRONO NE/J007196/1. The work was supported by the NERC Radiocarbon Facility
(allocation numbers 1722.0613 and 1878.1014). Thanks are due to the staff at the NERC AMS
Laboratory, East Kilbride for carbon isotope measurements. We thank the officers and crew of
the RRS James Cook for their help with acquisition and the British Geological Survey for
vibrocore collection during the cruise JC106. We also thank Kasper Weilbach, Riccardo
Arosio, Catriona Purcell, Zoe Roseby, Kevin Schiele and Elke Hanenkamp for their scientific
support on the JC106 leg 2 cruise. Finally, thanks to Hans Petter Sejrup and two anonymous
reviewers who provided detailed comments and suggestions to improve the manuscript.

References

- Andersen, K.K., Svensson, A., Johnsen, S.J., Rasmussen, S.O., Bigler, M., Röthlisberger, R.,
Ruth, U., Siggaard-Andersen, M-L., Steffensen, J.P., Dahl-Jensen, D., Vinther, B.M.,
Clausen, H.B., 2006. The Greenland Ice Core Chronology 2005, 15-42ka. Part 1:
constructing the time scale. *Quaternary Science Reviews*, 25, 3246-3257.
- Alley, R.B., Anandakrishnan, S., Dupont, T.K., Parizek, B.R., Pollard, D., 2007. Effect of
sedimentation on Ice-Sheet Grounding-Line Stability. *Science*, 315, 1838-1841.

795 Armishaw, J.E., Holmes, R.W., Stow, D.A.V., 1998. Morphology and sedimentation on the
 796 Hebrides Slope and Barra Fan, NW UK continental margin. Geological Society of London,
 797 Special publication, 129, 81-104.

798 Austin, W.E.N., Bard, E., Hunt, J.B., Kroon, D., Peacock, J.D., 1995. The ^{14}C age of the
 799 Icelandic Vedde Ash: implications for Younger Dryas marine reservoir age corrections.
 800 Radiocarbon, 37, 53-62.

801 Ballantyne, C.K., Ó Cofaigh, C., 2016. The last Irish Ice Sheet: Extent and Chronology. In
 802 Coxon, P., McCarron, S., Mitchell, F., (eds). Advances in Irish Quaternary Studies, vol 1,
 803 Atlantic Press, Paris. Pp101-149

804 Batchelor, C.L., Dowdeswell, J.A., Hogan, K.A., 2011. Late Quaternary ice flow and sediment
 805 delivery through Hinlopen Trough, Northern Svalbard margin: Submarine landforms and
 806 depositional fan. Marine Geology, 284, 13-27.

807 Batchelor, C.L., Dowdeswell, J.A., 2015. Ice-sheet grounding-zone wedges (GZWs) on high-
 808 latitude continental margins. Marine Geology, 363, 65-92.

809 Benetti, S., Dunlop, P. and Ó Cofaigh, C. (2010). Glacial and glacially-related features on the
 810 continental margin of northwest Ireland mapped from marine geophysical data. Journal of
 811 Maps, v. 2010, 14-29.

812 Bradwell, T., Stoker, M.S., Golledge, N.R., Wilson, C.K., Merritt, J.W., Long, D., Everest,
 813 J.D., Hestvik, O.B., Stevenson, A.G., Hubbard, A.L., Finlayson, A.G., Mathers, H.E.,
 814 2008. The northern sector of the last British Ice Sheet: Maximum extent and demise.
 815 Earth-Science Reviews, 88, 207-226.

816 Bradwell, T., Small, D., Fabel, D., Smedley, R.K., Clark, C.D., Saher, M.H., Callard, S.L.,
 817 Chiverrell, R.C., Dove, D., Moreton, S.G., Roberts, D.H., Duller, G.A.T., Ó Cofaigh, C.,
 818 2019. Ice-stream demise dynamically conditioned by trough shape and bed strength.
 819 Science Advances, 5, eaau1380.

820 Brinkerhoff, D., Truffer, M., Aschwanden, A., 2017. Sediment transport drives tidewater
821 glacier periodicity. *Nature Communications*, 8, 1-8.

822 Callard, S.L., Ó Cofaigh, C., Benetti, S., Chiverrell, R.C., van Landeghem, K., Saher, M.,
823 Gales, J., Small, D., Clark, C.D., Livingstone, S.J., and Fabel, D. (2018). Extent and
824 retreat history of the Barra Fan Ice Stream offshore western Scotland and northern Ireland
825 during the last glaciation. *Quaternary Science Reviews*, 201, 280-302.

826 Chiverrell, R.C., Thrasher, I.M., Thomas, G.S.P., Lang, A., Scourse, J.D., van Landeghem,
827 K.J., McCarroll, D., Clark, C.D., Ó Cofaigh, C., Evans, D.J.A., and Ballantyne, C.K.
828 (2013). Bayesian modelling the retreat of the Irish Sea Ice Stream. *Journal of Quaternary*
829 *Science*, 28, 200-209.

830 Chiverrell, R.C., Smedley, R.K., Small, D., Ballantyne, C.K., Burke, M.J., Callard, S.L.,
831 Clark, C.D., Duller, G.A.T., Evans, D.J.A., Fabel, D., van Landeghem, K., Livingstone, S.,
832 Ó Cofaigh, C., Thomas, G.S.P., Roberts, D.H., Saher, M., Scourse, J.D., Wilson, P., 2018.
833 Ice margin oscillations during deglaciation of the northern Irish Sea Basin. *Journal of*
834 *Quaternary Science*, 33, 739-762.

835 Clark, P.U., Dyke, A.S., Shakrun, J.D., Carlson, A.E., Clark, J., Wohlfarth, B., Mitrovica,
836 J.X., Hostetler, S.W., McCabe, A.M., 2009. The last glacial maximum. *Science*, 325, 710-
837 714

838 Clark, C.D., Hughes, A.L., Greenwood, S.L., Jordan, C. and Sejrup, H.P., 2012. Pattern and
839 timing of retreat of the last British-Irish Ice Sheet. *Quaternary Science Reviews*, 44, 112-
840 146.

841 Clark, C.D., Ely, J.C., Greenwood, S.L., Hughes, A.L.C., Meehan, R., Barr, I.D., Bateman,
842 M.D., Bradwell, T., Doole, J., Evans, D.J.A., Jordan, C.J., Monteys, X., Pellicer, X.M.,
843 Sheehy, M., 2018. BRITICE Glacial Map, version 2: a map and GIS database of glacial
844 landforms of the last British-Irish Ice Sheet. *Boreas*, 47, 11-27.

845 Cooper, J.A.G., Kelley, J.T., Belknap, D.F., Quinn, R., McKenna, J., 2002. Inner shelf
846 seismic stratigraphy off the north coast of Northern Ireland: new data on the depth of the
847 Holocene lowstand. *Marine Geology*, 186, 369-387.

848 Cowan, E.A., Polwell, R.D., 1990. Suspended sediment transport and deposition of cyclically
849 interlaminated sediment in a temperate glacial fjord, Alaska, USA. *Geological Society*,
850 London, Special Publications, 53, 75-89.

851 Cowan, E.A., Cai, J., Powell, R.D., Clark, J.D., Pitcher, J.N., 1997. Temperate glacimarine
852 varves: an example from Disenchantment Bay, Southern Alaska. *Journal of sedimentary*
853 *Research*, 3, 536-549

854 Domack, E.W., Harris, P.T., 1998. A new depositional model for ice-shelves, based upon
855 sediment cores from the Ross Sea and the Mac. Robertson shelf. *Antarctica. Annals of*
856 *Glaciology*, 27, 281-284

857 Dowdeswell, J.A., Whittington, R.J., Marienfeld, P., 1994. The origin of massive diamicton
858 facies by iceberg rafting and scouring, Scoresby Sund, East Greenland. *Sedimentology*, 41,
859 21-35

860 Dowdeswell, J.A., Whittington, R.J., Jennings, A.E., Andrews, J.T., Mackensen, A.,
861 Marienfeld, P., 2000. An origin for laminated glacimarine sediments through sea-ice build-
862 up and suppressed iceberg rafting. *Sedimentology*, 47, 557-576.

863 Dowdeswell, J.A., Ó Cofaigh, C., Pudsey, C.J., 2004. Continental slope morphology and
864 sedimentary processes at the mouth of an Antarctic palaeo-ice stream. *Marine Geology*, 204,
865 203-214.

866 Dowdeswell, J.A., Evans, J., O Cofaigh, C., 2010. Submarine landforms and shallow acoustic
867 stratigraphy of a 400 km-long fjord-shelf-slope transect, Kangerlussuaq margin, East
868 Greenland. *Quaternary Science Reviews*, 29, 3359-3369.

869 Dunlop, P., Shannon, R., McCabe, M., Quinn, R., and Doyle, E., 2010. Marine geophysical
 870 evidence for ice sheet extension and recession on the Malin Shelf: new evidence for the
 871 western limits of the British Irish Ice Sheet. *Mar. Geol.* 276 (1), 86-99.

872 Dunlop, P., Sacchetti, F., Benetti, S. and Ó Cofaigh, C. (2011). Mapping Ireland's glaciated
 873 continental margin using marine geophysical data. In: *Geomorphological Mapping: Methods and Applications: A Professional Handbook of Techniques and Applications*
 874 (Developments in Earth Surface Processes). (Eds: Smith, M.J, Paron, P. and Griffiths, J.S.),
 875 Elsevier pp. 337-355.

877 Evans, D.J.A., 2018. *Till: A glacial process sedimentology*. John Wiley and Sons Ltd, Oxford
 878 400p

879 Elverhøi, A., Norem, H., Andersen, E.S., Dowdeswell, J.A., Fossen, I., Haflidason, H.,
 880 Kenyon, N.H., Laberg, J.S., King, E.L., Sejrup, H.P., Solheim, A., Vorren, T., 1997. On
 881 the origin and flow behaviour of submarine slides on deep-sea fans on the Norwegian–
 882 Barents Sea continental margin. *Geo-Marine Letters*, 17, 119–125.

883 Eyles, N., Eyles, C.H., 1989. Glacially-influenced deep-marine sedimentation of the Late
 884 Precambrian Gaskiers Formation, Newfoundland, Canada. *Sedimentology*, 36, 601-620.

885 Greenwood, S.L., Clark, C.D., 2009. Reconstructing the last Irish Ice Sheet 2: a
 886 geomorphologically-driven model of ice sheet growth, retreat and dynamics. *Quaternary*
 887 *Science Reviews*, 28, 3101-3123.

888 Hesse, R., Khodabakhsh, S., Klauke, I. and Ryan, W.B.F., 1997. Asymmetrical turbid
 889 surface-plume deposition near ice-outlets of the Pleistocene Laurentide ice sheet in the
 890 Labrador Sea. *Geo-Marine Letters*, 17, 179-187.

891 Hogan, K.A., Dowdeswell, J., Ó Cofaigh,., 2012. Glacimarine sedimentary processes and
 892 depositional environments in an embayment fed by West Greenland ice streams. *Marine*
 893 *Geology*, 311, 1-16

894 Hogan, K.A., Ó Cofaigh, C., Jennings, A.E., Dowdeswell, J.A., Hiemstra, J.F., 2016.
 895 Deglaciation of a major palaeo-ice stream in Disko Trough, west Greenland. *Quaternary*
 896 *Science Reviews*, 147, 5-26.

897 Howe, J.A., Stoker, M.S., Wolfe, K.J., 2001. Deep-marine seabed erosion and gravel lags in
 898 the northwestern Rockall trough, North Atlantic Ocean. *Journal of the Geological Society*,
 899 158, 427-438.

900 Jennings, A.E., Andrews, J.T., Ó Cofaigh, C., St-Onge, G., Sheldon, C., Belt, S., Cabedo-
 901 Sanz, P., Pearce, C., Hillaire-Marcel, C., 2017. Ocean forcing of Ice Sheet retreat in
 902 central west Greenland from LGM to the early Holocene. *Earth and Planetary Science*
 903 *Letters*, 472, 1-13.

904 Jennings, A.E., Andrews, J.T., Ó Cofaigh, C., St-Onge, G., Belt, S., Cabedo-Sanz, P., Pearce,
 905 C., Hillaire-Marcel, C., Campbell, D.C., 2018. Baffin Bay paleoenvironments in the LGM
 906 and HS1: Resolving the ice-shelf question. *Marine Geology*, 402, 5-16.

907 Kilfeather, A.A., Ó Cofaigh, C., Lloyd, J.M., Dowdeswell, J.A., Xu, S., and Moreton, S.,
 908 2011. Ice stream retreat and ice shelf history in Marguerite Bay, Antarctic Peninsula:
 909 sedimentological and foraminiferal signatures. *Geological Society of America*
 910 *Bulletin*, 123, 997-1015.

911 King, E.L., Sejrup, H.P., Haflidason, H., Elverhøi, A., Aarseth, I., 1996. Quaternary seismic
 912 stratigraphy of the North Sea Fan: glacially-fed gravity flow aprons, hemipelagic
 913 sediments, and large submarine slides. *Marine Geology*, 130, 293-315.

914 Knutz, P.C., Austin, W.E.N., Jones, E.J.W., 2001. Millennial-scale depositional cycles
 915 related to British Ice Sheet variability and North Atlantic palaeocirculation since 45 kyr
 916 BP, Barra Fan, UK margin. *Paleoceanography*, 16, 53-64.

917 Knutz, P.C., Zahn, R., Hall, I.R., 2007. Centennial-scale variability of the British Ice Sheet:
 918 implications for climate forcing and Atlantic meridional overturning circulation during the
 919 last deglaciation. *Paleoceanography*, 22, PA1207.

920 Lloyd, J.M., Moros, M., Perner, K., Telford, R., Kujipers, A., Jansen, E., McCarthy, D.,
 921 2011. A 100 year record of ocean temperature control on the stability of Jakobshavn
 922 Isbrae, west Greenland. *Geology*, 39, 867-870.

923 Lucchi, R.G., Camerlenghi, A., Rebesco, M., Colmenero-Hidalgo, E., Sierro, F.J., Sagnotti,
 924 L., Urgeles, R., Melis, R., Morigi, C., Bárcena, M.-A., Giorgetti, G., Villa, G., Persico, D.,
 925 Flores, J.-A., Rigual-Hernández, A.S., Pedrosa, M.T., Macri, P., Carburlootto, A., 2013.
 926 Postglacial sedimentary processes on the Storfjorden and Kveithola trough mouth fans:
 927 Significance of extreme glacimarine sedimentation. *Global and Planetary Change*, 111,
 928 309-326.

929 Naylor, D., Shannon, P.M., Murphy, N., 1999. Irish Rockall Basin Region- A standard
 930 structural nomenclature system. *Special Publications*, 1/99

931 McCarron, S., Praeg, D., Ó Cofaigh, C., Monteys, X., Thébaudeau, B., Craven, K., Saqab,
 932 M.M., Cova, A., 2018. A Plio-Pleistocene sediment wedge on the continental shelf west of
 933 central Ireland: The Connemara Fan. *Marine Geology*, 1, 97-114.

934 Mugford, R.I., Dowdeswell, J.A., 2011. Modeling glacial meltwater plume dynamics and
 935 sedimentation in high-latitude fjords. *Journal of Geophysical Research*, 116,
 936 10.1029/2010JF001735.

937 Ó Cofaigh, C., Dowdeswell J.A., 2001. Laminated sediments in glacimarine environments:
 938 diagnostic criteria for their interpretation. *Quaternary Science Reviews*, 20, 1411-1436.

939 Ó Cofaigh, C., Dowdeswell, J.A., Allen, C.S.A., Hiemstra, J., Pudsey, C.J., Evans, J., Evans,
 940 D.J.A., 2005. Flow dynamics and till genesis associated with a marine-based Antarctic
 941 palaeo-ice stream. *Quaternary Science Reviews*, 24, 709-740.

942 Ó Cofaigh, C., Evans, D.J.A. and Hiemstra, J., 2011. Formation of a stratified subglacial “till”
 943 (glacitectonite) assemblage by ice-marginal thrusting and glacier overriding. *Boreas*, 40, 1-
 944 14.

945 Ó Cofaigh, C., Dunlop, P. and Benetti, S., (2012). Marine geophysical evidence for Late
 946 Pleistocene ice sheet extent and recession on the continental shelf off north-west Ireland.
 947 *Quaternary Science Reviews*, 44, 147-159.

948 Ó Cofaigh, C., Dowdeswell, J.A., Jennings, A.E., Hogan, K., Kilfeather, A., Hiemstra, J.F.,
 949 Noormets, R., Evans, J., McCarthy, D.J., Andrews, J.T., Lloyd, J.M., Moros, M., 2013. An
 950 extensive and dynamic ice sheet on the West Greenland shelf during the last glacial cycle.
 951 *Geology*, 41, 219-222.

952 Ó Cofaigh, C., Hogan, K., Dowdeswell, J.A., and Streuff, K. (2016). Stratified glacimarine
 953 basin-fills in West Greenland fjords. In: Dowdeswell, J.A., Canals, M., Jakobsson, M.,
 954 Todd, B.J., Dowdeswell, E.K. & Hogan, K.A. (eds.), *Atlas of Submarine Glacial*
 955 *Landforms: Modern, Quaternary and Ancient*. Geological Society, London, p. 99-100.

956 Ó Cofaigh, C., Weilbach, K., Lloyd, J., Benetti, S., Callard, S.L., Purcell, C., Chiverrell,
 957 R.C., Dunlop, P., Saher, M., Livingstone, S.J., Van Landeghem, K.J.J., Moreton, S.G.,
 958 Clark, C.D., Fabel, D., 2019. Early deglaciation of the British-Irish Ice Sheet on the
 959 Atlantic shelf northwest of Ireland driven by glacioistostatic depression and high relative
 960 sea level. *Quaternary Science Reviews*,

961 Reimer, P.J., Bard, E., Bayliss, A., Beck, J.W., Blackwell, P.G., Ramsey, C.B., Buck, H.,
 962 Cheng, H., Edwards, R.L., Friedrich, M., Grootes, P.M., Guilderson, T.P., Hafildason, H.,
 963 Hajdas, I., Hatté, C., Heaton, T.J., Hoffman, D.L., Hogg, A.G., Hughen, K.A., Kaiser,
 964 K.F., Kromer, B., McCormac, F.G., Manning, S.W., Nui, M., Reimer, R.W., Richards,
 965 D.A., Scott, E.M., Southon, J.R., Staff, R.A., Turney, C.S.M., van der Plicht, J., 2013.

966 Intcal13 and Marine13 radiocarbon age calibration curves, 0-50,000 years Cal Bp.
 967 Radiocarbon, 55, 1869-1887.

968 Peck, V.L., Hall, I.R., Zahn, R., Elderfield, H., Grousset, F., Hemming, S.R., Scourse, J.D.,
 969 2006. High resolution evidence for linkages between NW European ice sheet instability
 970 and Atlantic meridional overturning circulation. *Earth and Planetary Science Letters*, 243,
 971 476–488.

972 Peck, V.L., Hall, I.R., Zahn, R., Grousset, F., Hemming, S.R., Scourse, J.D., 2007. The
 973 relationship of Heinrich events and their European precursors over the past 60 ka BP: a
 974 multi-proxy ice-rafted debris provenance study in the north east Atlantic. *Quaternary
 975 Science Reviews*, 26, 862-875.

976 Peters, J.L., Benetti, S., Dunlop, P., Ó Cofaigh, C., 2015. Maximum extent and dynamic
 977 behaviour of the last British Irish ice sheet west of Ireland. *Quaternary Science Reviews*,
 978 128, 48-68.

979 Peters, J.L., Benetti, S., Dunlop, P., Ó Cofaigh, C., Moreton, S.G., Wheeler, A.J., Clark,
 980 C.D., 2016. Sedimentology and chronology of the advance and retreat of the last British-
 981 Irish Ice Sheet on the continental shelf west of Ireland. *Quaternary Science Reviews*, 140,
 982 101-124.

983 Plets, R.M.K., Callard, S.L., Cooper, J.A.G., Long, A.J., Quinn, R.J., Belknap, D.F.,
 984 Edwards, R.J., Jackson, D.W.T., Kelley, J.T., Long, D., Milne, G.A., Monteys, X., 2015.
 985 *Marine Geology*, 369, 251-272.

986 Powell, R.D., 1991. Grounding-line systems as second-order controls on fluctuations of
 987 tidewater termini of temperate glaciers, *in* Anderson, J.B., Ashley, G.M., eds. *Glacial
 988 marine sedimentation: Palaeoclimatic significance*. Boulder, Geological Society of
 989 America Special Paper 261, 75-93.

990 Powell, R.D., and Domack, E.W., 1995. Modern glaciomarine environments. In: Menzies, J.
 991 (ed.), *Glacial Environments*, vol. 1: Modern Glacial Environments: Processes, Dynamics
 992 and Sediments. Butterworth-Heinemann, Oxford, 445-486.

993 Praeg, D., McCarron, S., Dove, D., Ó Cofaigh, C., Scott, G., Monteys, X., Facchin, L.,
 994 Romeo, R., Coxon, 2015. Ice sheet extension to the Celtic Sea shelf edge at the Last
 995 Glacial Maximum. *Quaternary Science Reviews*, 111, 107-112.

996 Roberts, D.H., Evans, D.J.A., Callard, S.L., Clark, C.D., Bateman, M.D., Medialdae, A.,
 997 Dove, D., Cotterill, C.J., Saher, M., Ó Cofaigh, C., Chiverrell, R.C., Moreton, S.G., Fable,
 998 D., Bradwell, T., 2018. Ice marginal dynamics of the last British-Irish Ice Sheet in the
 999 southern North Sea: Ice limits, timing and the influence of the Dogger Bank. *Quaternary*
 1000 *Science Reviews*, 198, 181-207.

1001 Sacchetti, F., Benetti, S., Ó Cofaigh, C. and Georgiopoulou, A., 2012. Geophysical evidence
 1002 of deep-keeled icebergs on the Rockall Bank, Northeast Atlantic Ocean. *Geomorphology*,
 1003 159-160, 63-72.

1004 Scourse, J.D., Haapaniemi, A.I., Colmenero-Hildago, E., Peck, V.L., Hall, I.R., Austin,
 1005 W.E.N., Knutz, P.C., Zahn, R., 2009. Growth, dynamics and deglaciation of the last
 1006 British-Irish ice sheet: the deep-sea ice-rafted detritus record. *Quaternary Science*
 1007 *Reviews*, 28, 3066-3084.

1008 Scourse, J.D., Saher, M., Van Landeghem, K.J.J., Lockhart, E., Purcell, C., Callard, L.,
 1009 Roseby, Z., Allinson, B., Pieńkowski, Ó Cofaigh, C., Praeg, D., Ward, S., Chiverrell, R.,
 1010 Moreton, S., Fabel, D., Clark, C.D., 2019. Advance and retreat of the marine-terminating
 1011 Irish Sea Ice Stream into the Celtic Sea during the last glacial: Timing and maximum
 1012 extent. *Marine Geology*, 412, 55-68.

1013 Sejrup, H.P., Hjelstuen, B.O., Torbjørn Dahlgren, K.I., Haflidason, H., Kuijpers, A., Nygård,
 1014 A., Praeg, D., Stoker, M.S., Vorren, T.O., 2005. Pleistocene glacial history of the NW
 1015 European continental margin. *Marine and Petroleum Geology*, 22, 1111-1129.
 1016 Sejrup, H.P., Clark, C.D., Hjelstuen, B.O., 2016. Rapid ice sheet retreat triggered by ice
 1017 stream debuitressing: Evidence from the North Sea. *Geology*, 44, 355-358.
 1018 Shipp, S.S., Wellner, J.S., Anderson, J.B., 2002. Retreat signature of a polar ice stream: sub-
 1019 glacial geomorphic features and sediment from the Ross Sea, Antarctica, Special
 1020 Publication-Geological Society of London, 203, 277-304.
 1021 Siddall, M., Rohling, E.J., Almogi-Labin, A., Hemleben, C., Meischner, D., Schmelzer, I.,
 1022 Smeed, D.A., 2003. Sea-level fluctuations on the last glacial cycle. *Nature*, 423, 853-858.
 1023 Singarayer, J.S., Richards, D.A., Ridgwell, A., Valdes, P.J., Austin, W.E.N., Beck, J.W.,
 1024 2008. An oceanic origin for the increase of atmospheric radiocarbon during the Younger
 1025 Dryas. *Geophysical Research Letters*, 35, L14707.
 1026 Small, D., Austin, W., Rinterknecht, V., 2013a. Freshwater influx, hydrographic
 1027 reorganization and the dispersal of ice-rafted detritus in the sub-polar North Atlantic
 1028 Ocean during the last deglaciation. *Journal of Quaternary Science*, 28, 527-535.
 1029 Small, D., Smedley, R.K., Chiverrell, R.C., Scourse, J.D., Ó Cofaigh, C., Duller, G.A.T.,
 1030 McCarron, S., Burke, M.J., Evans, D.J., Fabel, D., Gheorghiu, D.M., Thomas, G.S.P., Xu,
 1031 S., Clark, C.D., 2018. Trough geometry was a greater influence than climate-ocean forcing
 1032 in regulating retreat of the marine-based Irish-Sea Ice Stream. *Bulletin of the Geological*
 1033 *Society of America*, 130, 1981-1999.
 1034 Smedley, R.K., Scourse, J.D., Small, D., Hiemstra, J.F., Duller, G.A.T., Bateman, M.D.,
 1035 Burke, M.J., Chiverrell, R.C., Clark, C.D., Davies, S.M., Fabel, D., Gheorghiu, D.M.,
 1036 McCarroll, D., Medialdea, A., Xu, S., 2017. New age constraints for the limit of the
 1037 British-Irish Ice Sheet on the Isles of Scilly. *Journal of Quaternary Science*, 32, 48–62.

1038 Stow, D.A.V., Shanmugam, G., 1980. Sequence of structures in fine-grained turbidites:
1039 comparison of recent deep-sea and ancient flysch sediments. *Sedimentary Geology*, 25,
1040 23-42.

1041 Stow, D.A.V., Piper, D.J.W., 1984. Deep-water fine-grained sediments: facies models.
1042 Geological Society, London, Special Publication, 15, 611-646.

1043 Stravers, J.A., Powell, R.D., 1997. Glacial debris flow deposits on the Baffin Island shelf:
1044 seismic facies architecture of till-tongue-like deposits. *Marine Geology*, 143, 151-168.

1045 Thébaudeau, B., Monteys, X., McCarron, S., O'Toole, R., Caloca, S., 2016. Seabed
1046 geomorphology of the Porcupine Bank, west of Ireland. *Journal of Maps*, 12, 947-958.

1047 Todd, B.J., Valentine, P.C., Longva, O., Shaw, J., 2007. Glacial landforms on the German
1048 Bank, Scotian Shelf: evidence for Late Wisconsinan ice-sheet dynamics and implication
1049 for the formation of De Geer moraines. *Boreas*, 36, 148-169.

1050 Van Landegham, K.J.J., Wheeler, A.J., Mitchell, N.C., 2009. Seafloor evidence for palaeo-
1051 ice streaming and calving of the grounded Irish Sea Ice Stream: implications for the
1052 interpretation of its final deglaciation phase. *Boreas*, 38, 119-131.

1053 Vianna, A.R., Faugères, J-C., Stow, D.A.V., 1988. Bottom current controlled sand deposits- a
1054 review of modern shallow to deep-water environments. *Sedimentary Geology*, 115, 53-80.

1055 Wanamaker Jr, A.D., Butler, P.G., Scourse, J.D., Heinemeier, J., Eiríksson, J., Knudsen,
1056 K.L., Richardson, C.A., 2012. Surface changes in the North Atlantic meridional
1057 overturning circulation during the last millennium. *Nature communications*, 3, 899.

1058 Wellner, J., Lowe, A., Shipp, S., Anderson, J., 2001. Distribution of glacial geomorphic
1059 features of the Antarctic continental shelf and correlation with substrate: implications for
1060 ice behaviour. *Journal of Glaciology*, 158, 397-411

1061 Woodworth-Lynas, C.M.T., Dowdeswell, J.A., 1994. Soft-sediment striated surfaces and
1062 massive diamicton facies produced by floating ice. In: Deynoux, M., Miller, J.M.G.,

Domack, E.W., Eyles, N., Fairchild, I.J., Young, G.M., (Eds.), *Earth's Glacial Record*.
Cambridge University Press, Cambridge, 241-259.

Figures:

Figure 1: Location map with a) Regional schematic map showing the maximum extent of the British Irish Ice Sheet during the last glacial, modified from Peters et al. (2015) with ice-marginal and Donegal Barra Fan positions previously published by Armishaw et al. (2000), Knutz et al. (2001), Benetti et al. (2010), Dunlop et al.(2010), Ó Cofaigh et al. (2012), Sacchetti et al. (2012), Thébaudeau et al. (2016) and Clark et al. (2018) and b) Galway Bay continental shelf showing the labelled core locations (red circles) and seismic profiles shown in Figs 2, and 7 (black lines labelled).

Figure 2: Seismic lines that span the mid-shelf trough to mid-shelf with a) in the north and b) in the south of the shelf.

Figure 3: a) close up of the seismic line over core sites 194VC-196VC with interpretation panel underneath, the vertical red lines mark the core location and penetration. Note the seabed artefact visible in the top right-hand side of this image b) core logs for core 196VC, 195VC and 194VC, with calibrated radiocarbon dates, shear strength measurements in kPa and lithofacies codes with colour representing the associated acoustic unit in the interpretation panel above.

Figure 4: Close-up seismic images from the northern line, with a) the seismic data and interpretation panel covering mounds 1 to 3 (M1-3) described in section 4.1, b) seismic data

and interpretation panel for cores locations 191VC and 190VC, and c) seismic data and interpretation panel for Mound 5 and core location 186VC. The vertical red lines mark the core location and penetration.

Figure 5: Close-up seismic image and interpretation panel of mounds 5 to 6 identified in the southern line and described in section 4.1. The vertical red lines mark the core location and penetration.

Figure 6: core logs for all cores collected on the mid-shelf, with calibrated radiocarbon dates, shear strength measurements in kPa and lithofacies codes with colour representing the associated acoustic unit in the interpretation panel of Figures 4 and 5.

Figure 7: Seismic lines from offshore Connemara coastline, inner-shelf, with a) a 23 km long seismic line with interpretation panel of the seismic data below, and b) close-up of the seismic data and interpretation panel for cores 184VC to 181VC. The vertical red lines on mark the core location and penetration.

Figure 8: Core logs of cores collected in the inner-shelf offshore the Connemara coast with calibrated radiocarbon dates, shear strength measurements in kPa and lithofacies codes with colour representing the associated acoustic unit in Figure 7.

Figure 9: Example core photograph and x-radiographs of the different lithofacies described in section 4.3. The white dashed lines mark stratigraphic boundaries.

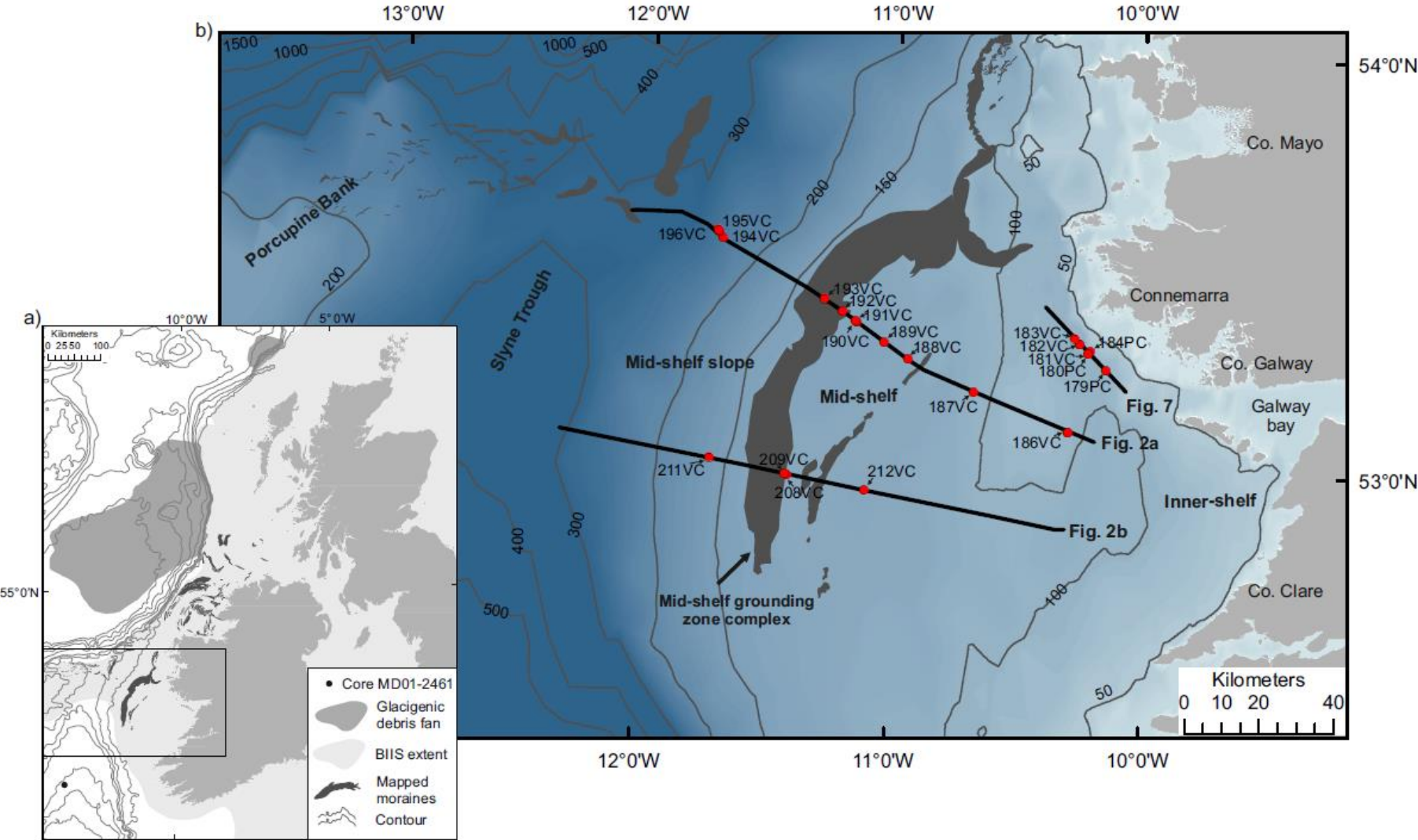
Figure 10: Time-distance diagram of ice-sheet extent on the continental shelf offshore Galway Bay from the Last Glacial Maximum (LGM) to 17 ka BP. The position of the ice sheet margin is shown as a solid black line with the dashed line representing periods of retreat. The shelf-edge position at 27-26 ka BP is implied from the IRD records of Peck et al. (2006, 2007), whilst the mid-shelf margins are based on radiocarbon dates in this study and from Peters et al. (2016). Double-ended arrows represent the oscillating ice margin on the mid-shelf

Tables

Table 1. Location, water depth and core recovery of cores collected from Galway Bay

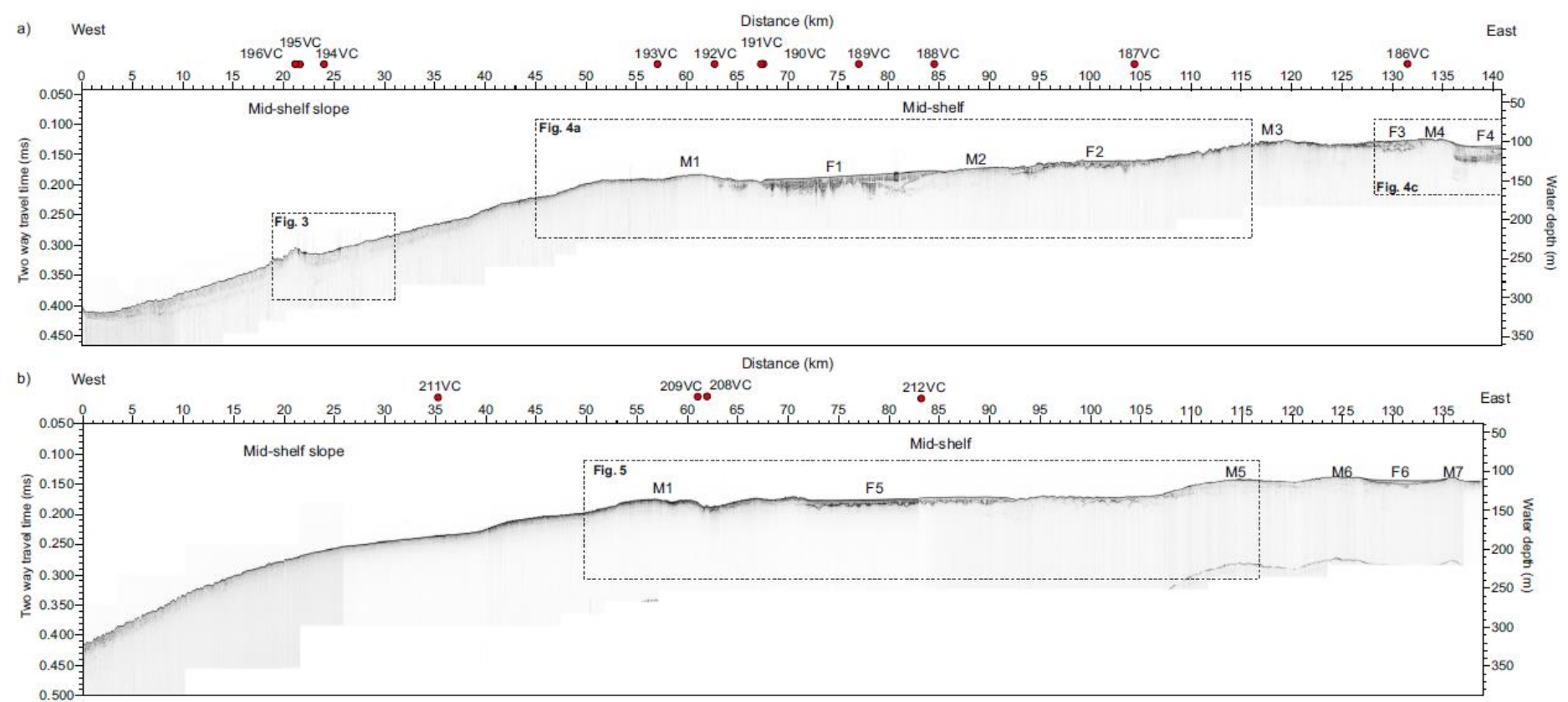
Table 2. Radiocarbon results for cores discussed in this study

1135 Figure 1



1136

1137 Figure 2



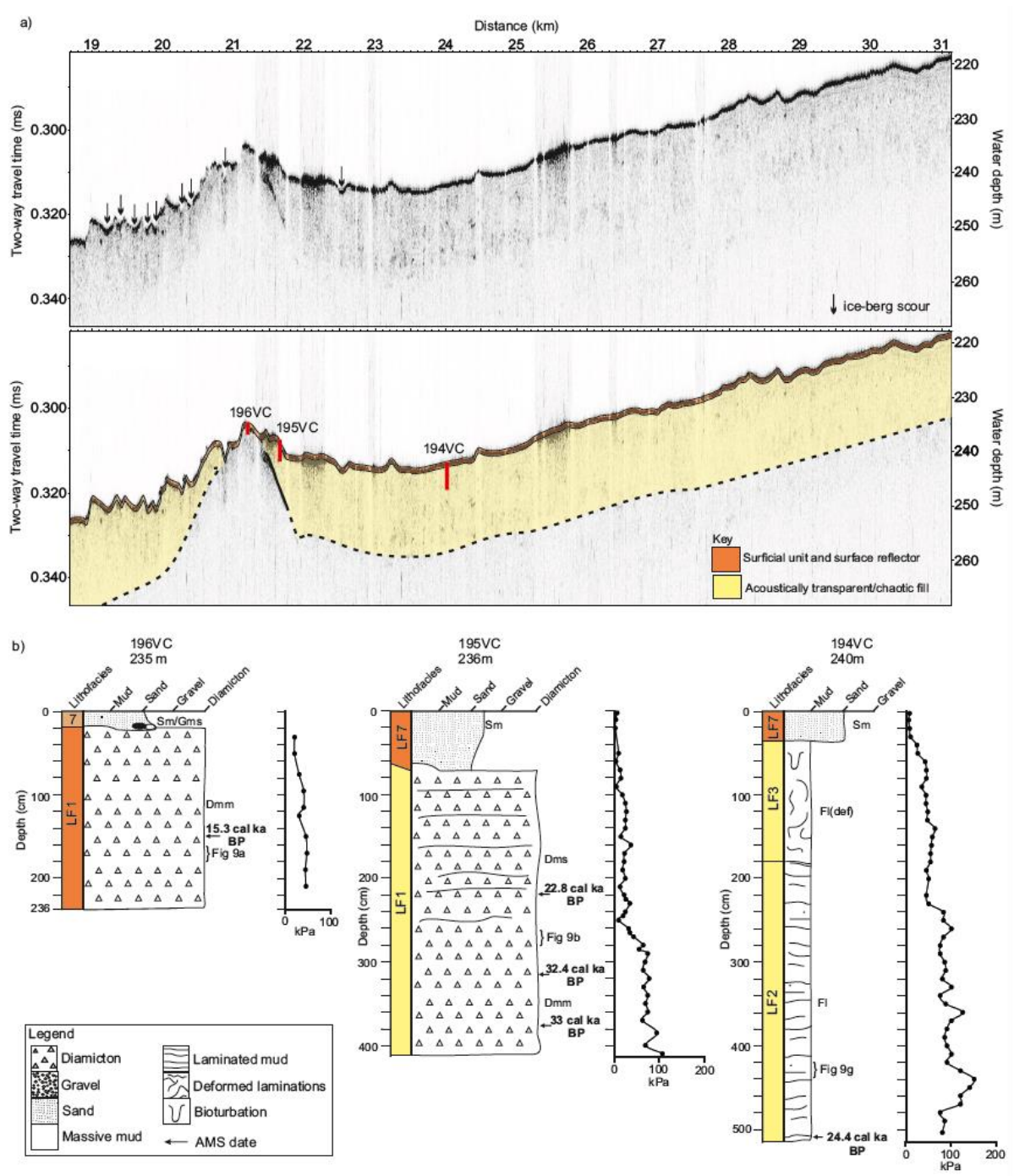
1138

1139

1140

1141

1142 Figure 4



1143

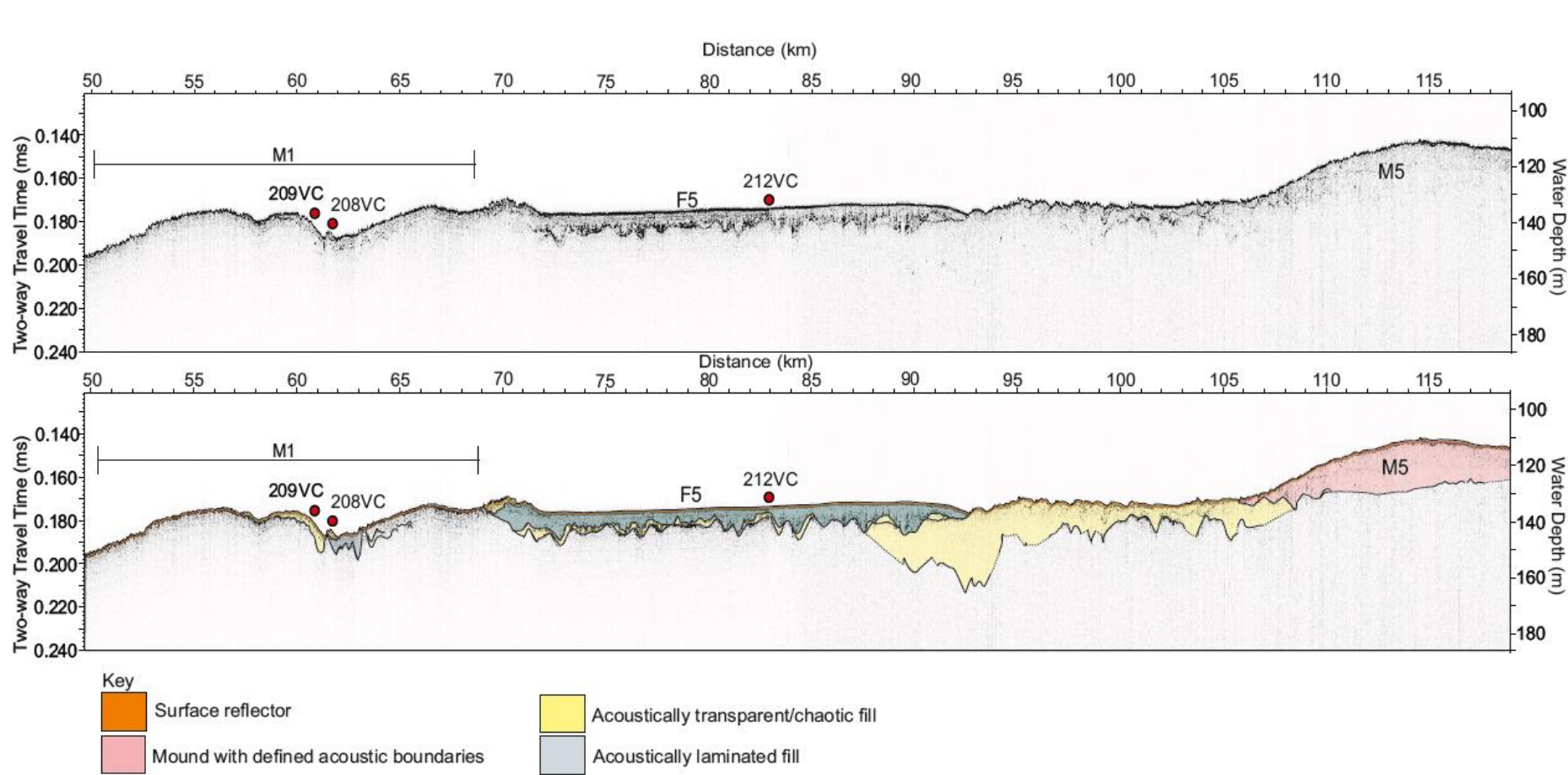
1144

1145

1146

1147

1148 Figure 5



1149

1150

1151

Figure 6

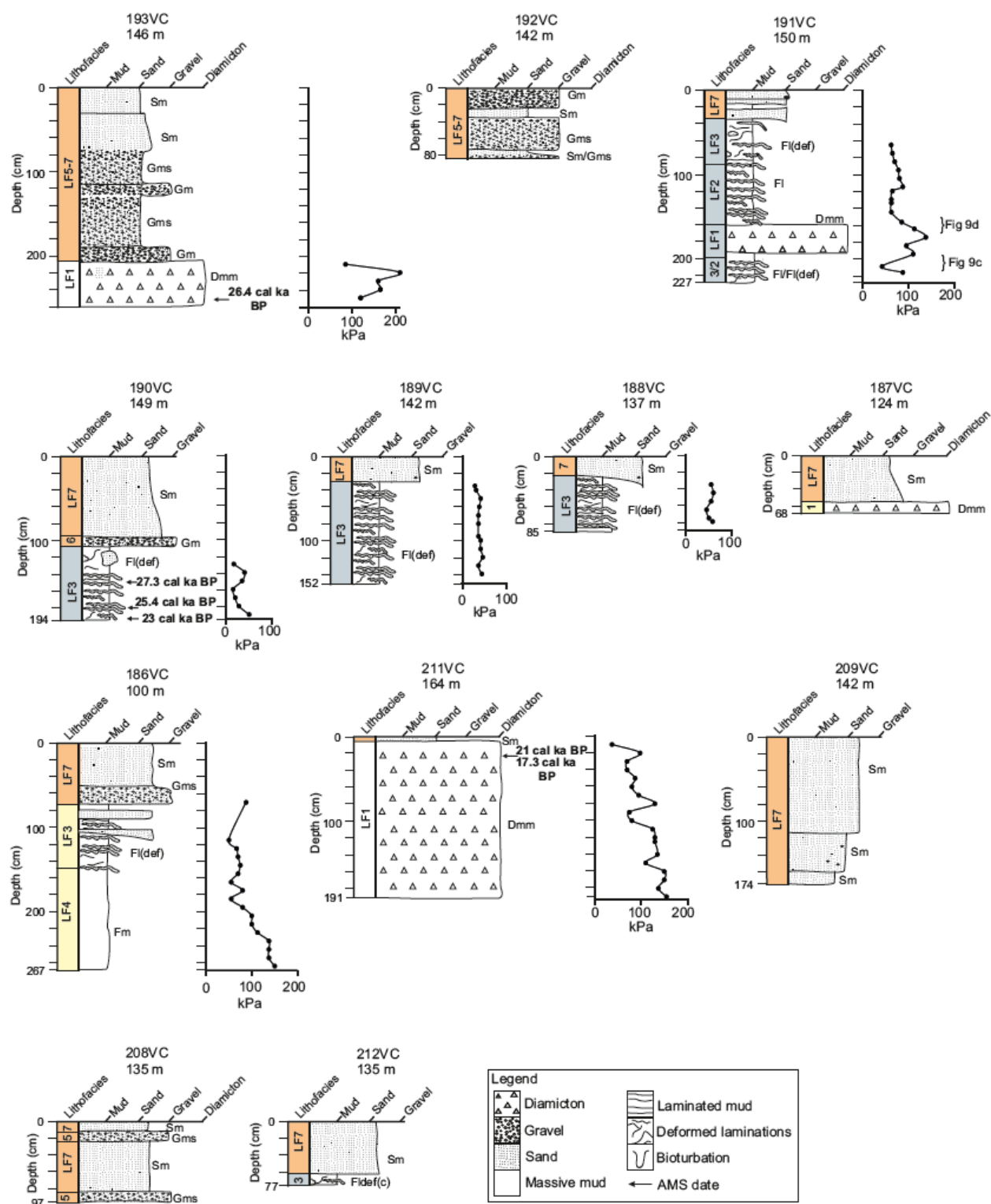


Figure 7

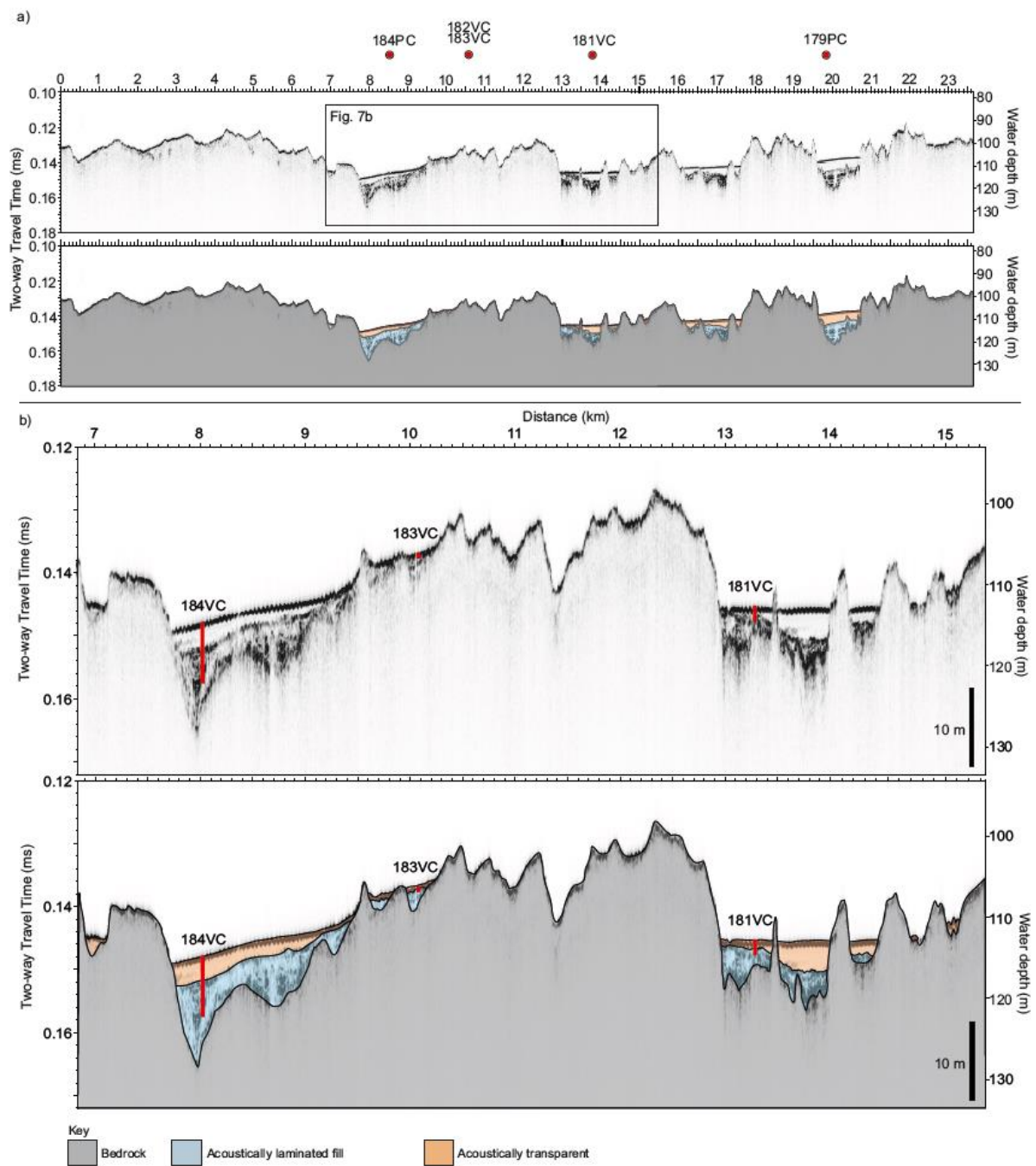


Figure 8

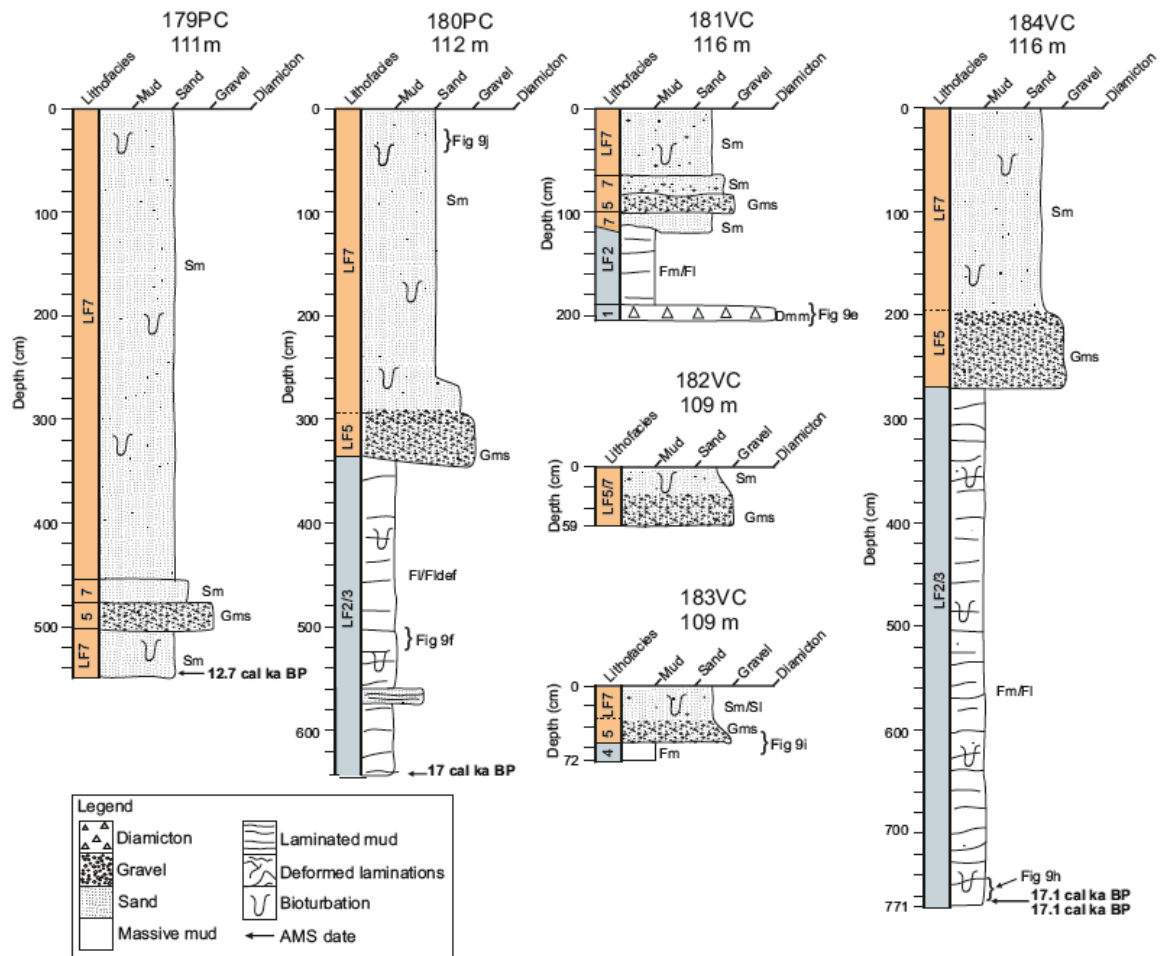


Figure 9

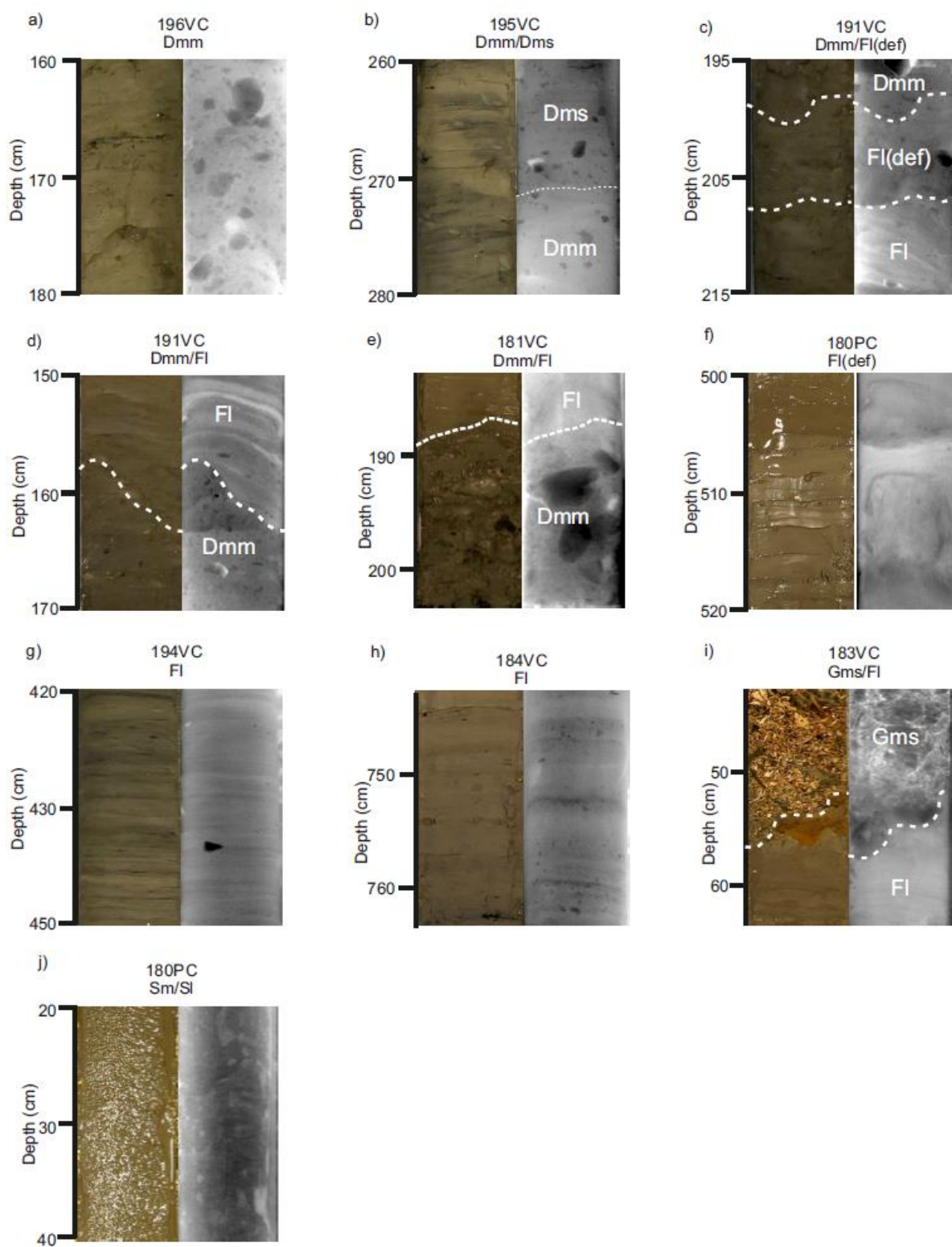
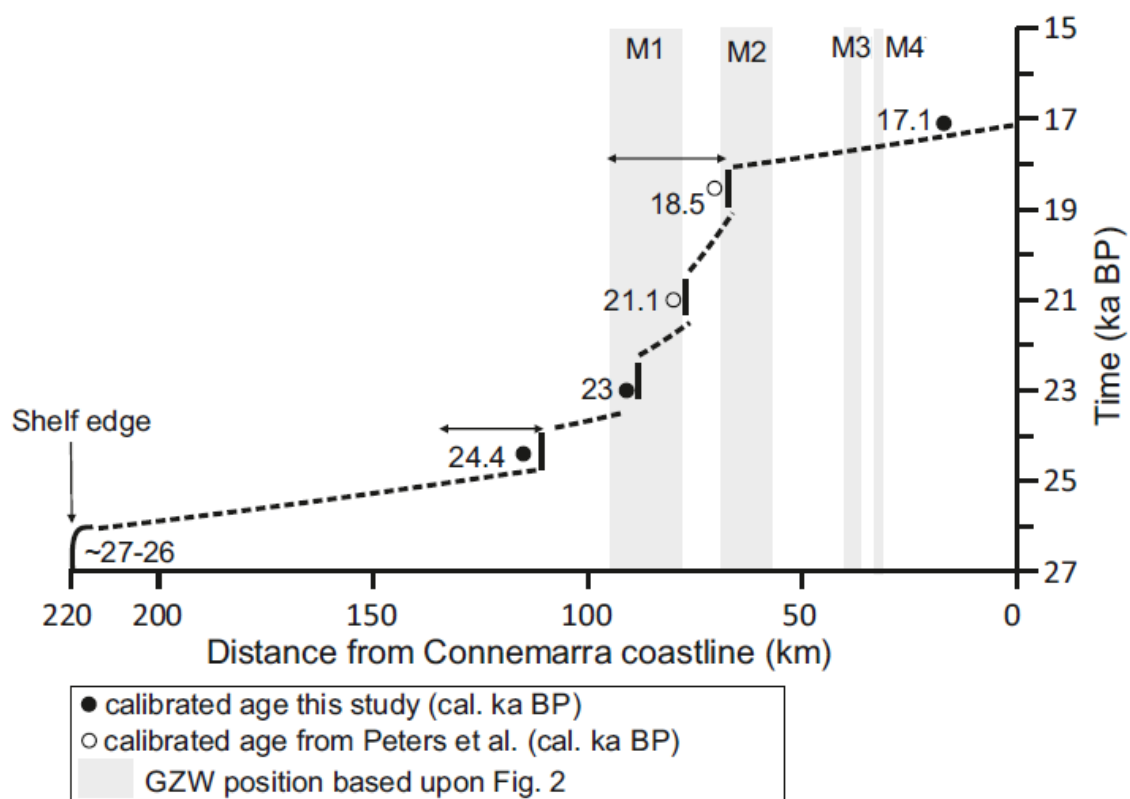
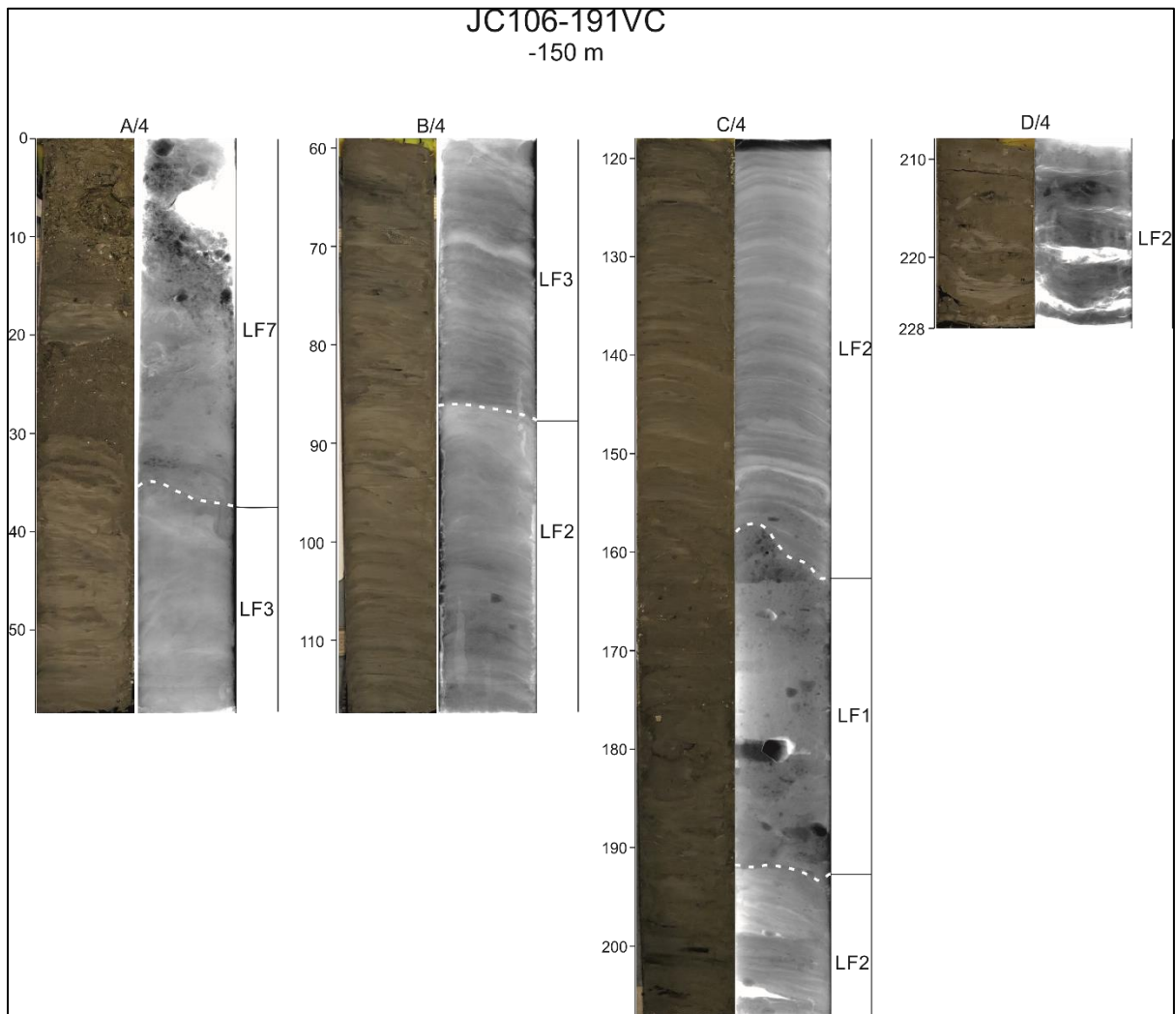


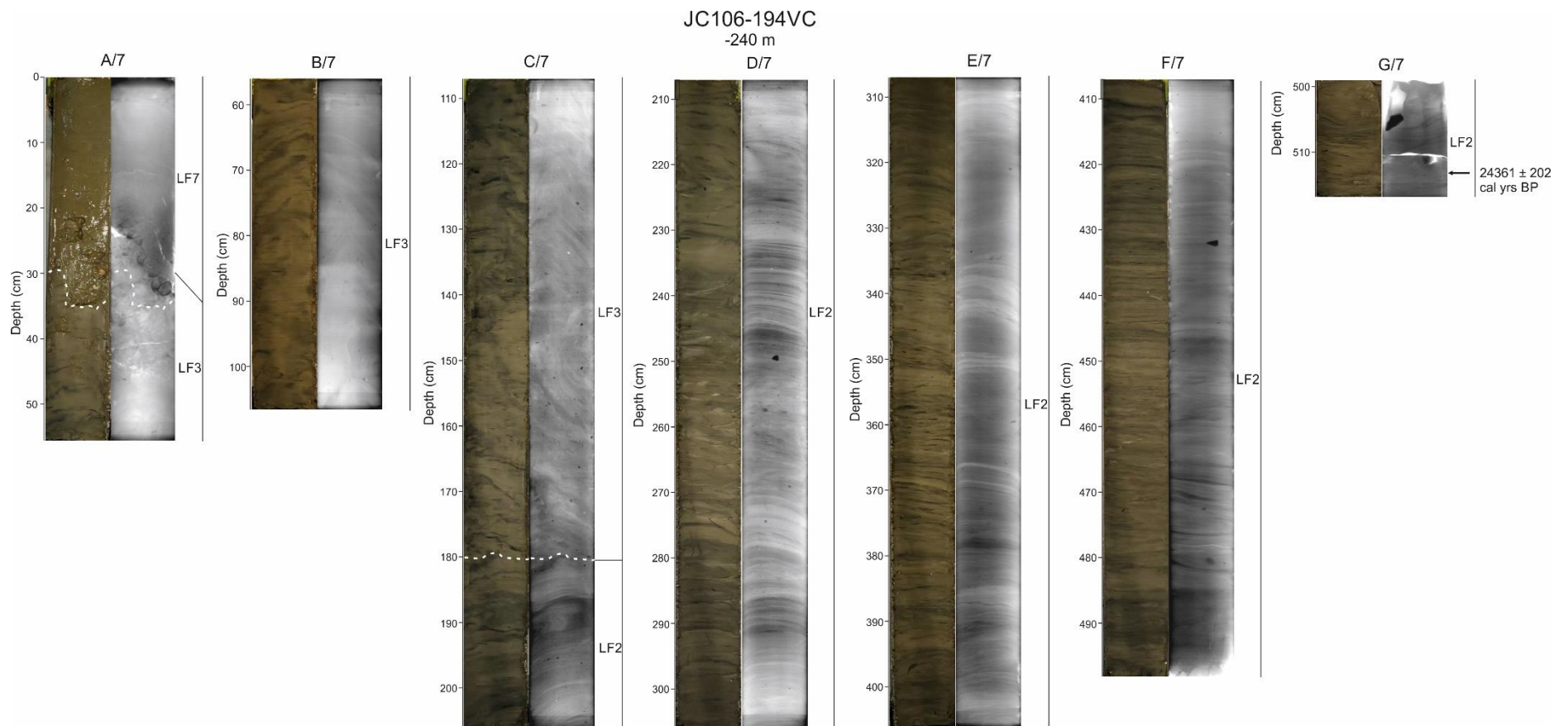
Figure 10



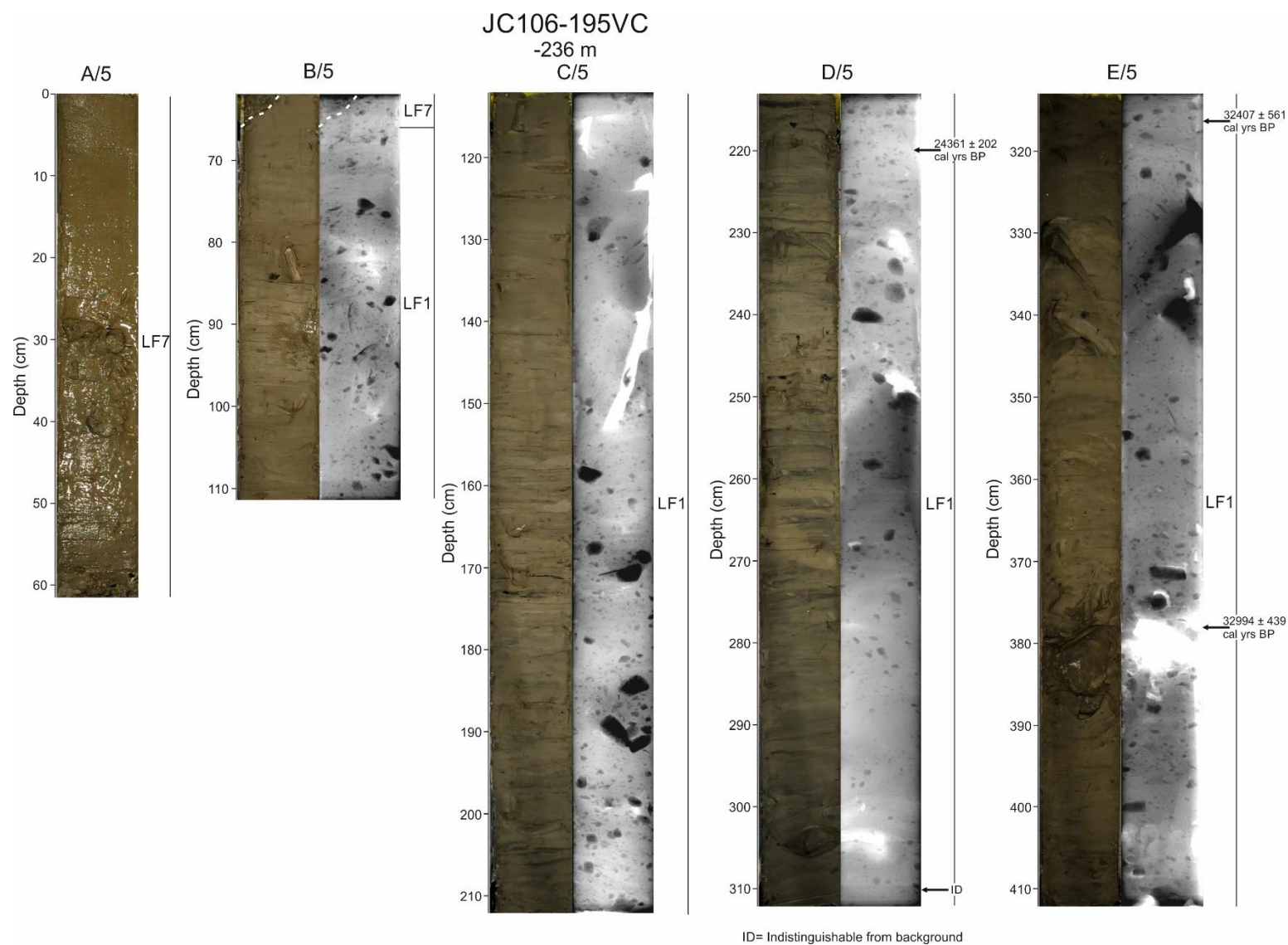
Supplementary Information



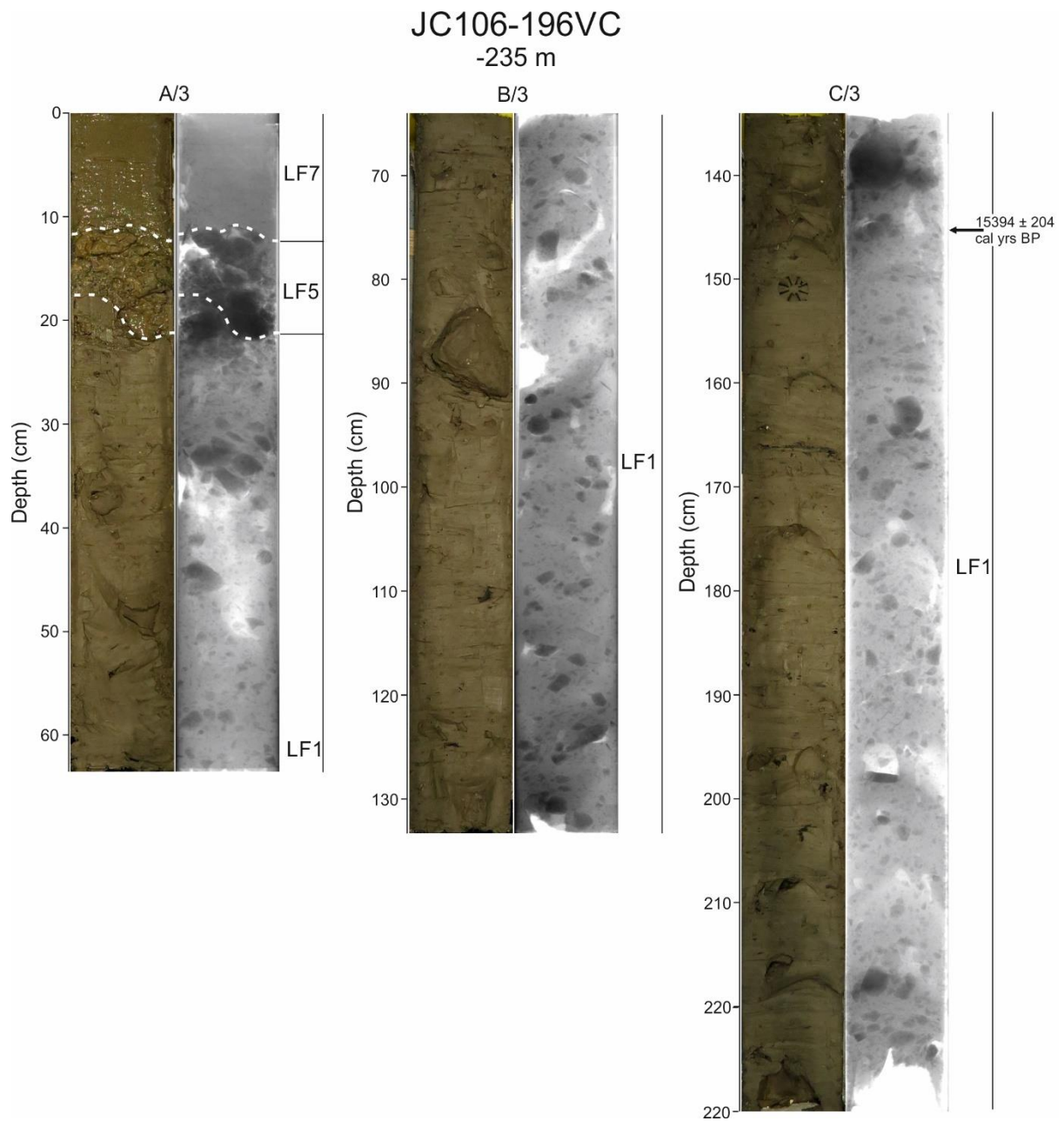
Supplementary Figure 1: X-radiograph and photograph of core 191VC with lithofacies interpretations mentioned in section 4.2 written alongside.



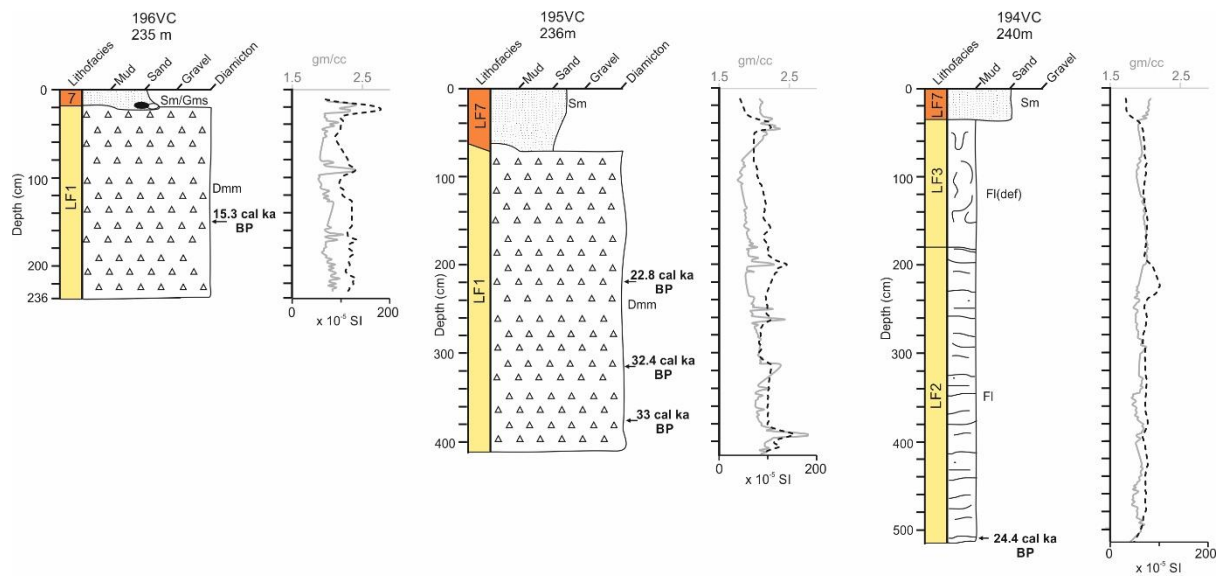
Supplementary Figure 2: X-radiograph and photograph of core 194VC with core lithofacies mentioned in section 4.2 written alongside.



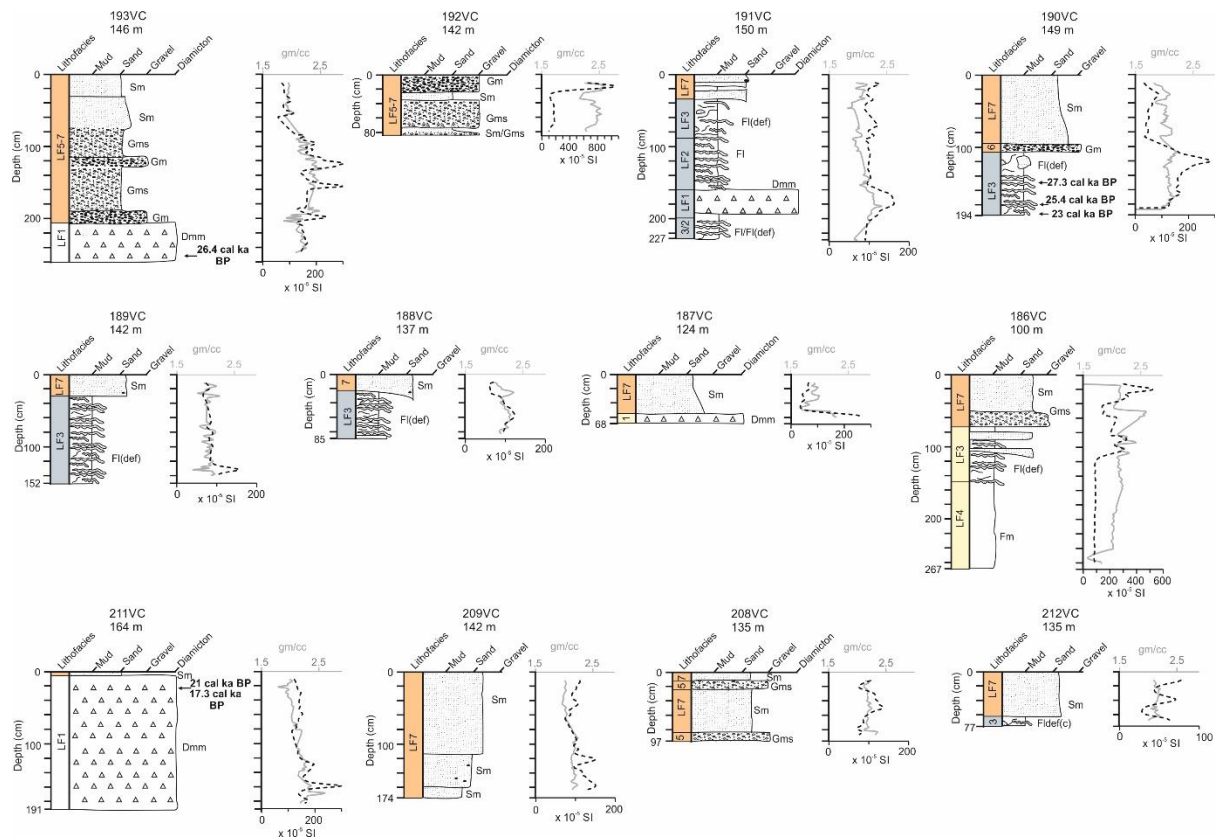
Supplementary Figure 3: X-radiograph and photograph of core 195VC with lithofacies interpretations mentioned in section 4.2 written alongside.



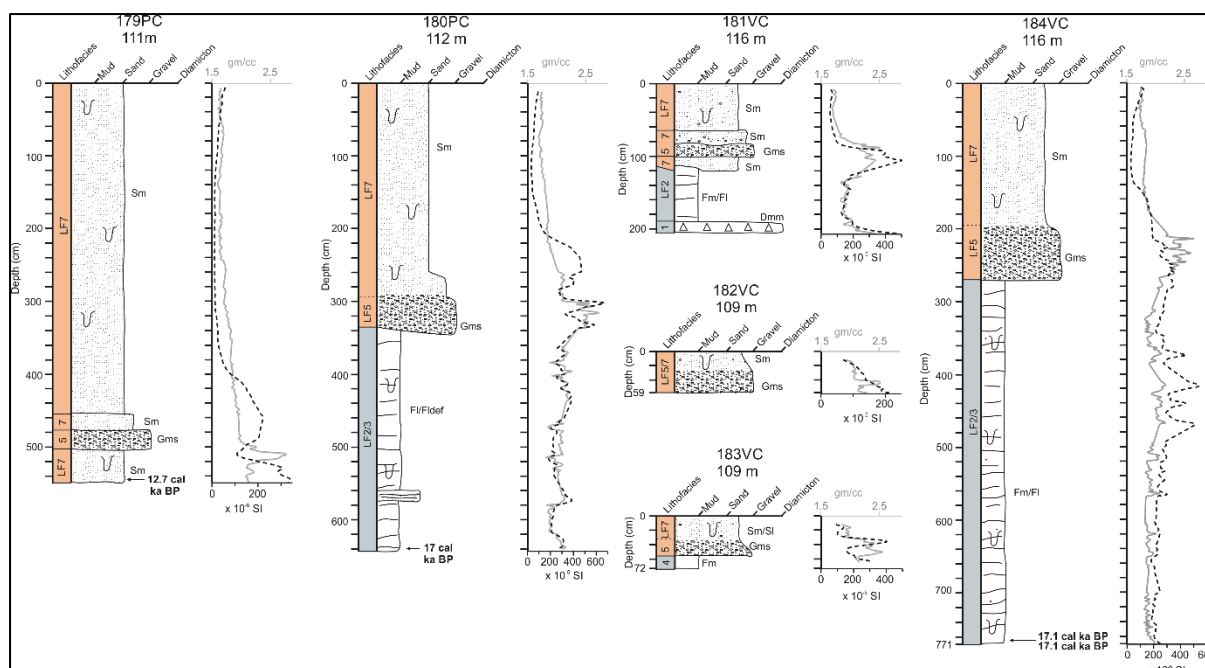
Supplementary Figure 4: X-radiograph and photograph of core 196VC with lithofacies interpretations mentioned in section 4.2 written alongside.



Supplementary Figure 5: Core logs for core 196VC, 195VC and 194VC, with calibrated radiocarbon dates and lithofacies codes with colour representing the associated acoustic unit shown in Figure 3a. The graph alongside the core logs present the wet bulk densities results (solid grey line) and magnetic susceptibility results (black dashed line).



Supplementary Figure 6: Core logs for all cores collected on the mid-shelf, with calibrated radiocarbon dates, and lithofacies codes with colour representing the associated acoustic unit in the interpretation panel of Figures 4 and 5. The graph alongside the core logs present the wet bulk densities results (solid grey line) and magnetic susceptibility results (black dashed line). Note the magnetic susceptibility scale changes between cores.



Supplementary Figure 7: Core logs of cores collected in the inner-shelf offshore the Connemara coast with calibrated radiocarbon dates, and lithofacies codes with colour representing the associated acoustic unit in Figure 7. The graph alongside the core logs present the wet bulk densities results (solid grey line) and magnetic susceptibility results (black dashed line). Note the magnetic susceptibility scale changes between cores.

50

51

52